Geophys. J. Int. (2002) **151,** 427–451

Derivation of a microstructural poroelastic model

Mark Chapman,[1,2] Sergei V. Zatsepin[1] and Stuart Crampin[1,2]

[1]*Department of Geology and Geophysics, University of Edinburgh Grant Institute, West Mains Road, Edinburgh* EH9 3JW, *UK*
[2]*Edinburgh Anisotropy Project, British Geological Survey, Murchison House, West Mains Road, Edinburgh* EH9 3LA, *UK. E-mail: m.chapman@bgs.ac.uk*

Accepted 2002 May 14. Received 2002 May 3; in original form 2001 July 25

SUMMARY

The standard description of wave propagation in fluid-saturated porous media is given by the Biot–Gassmann theory of poroelasticity. The theory enjoys strong experimental support, except for specific and systematic failings. These failings may be addressed by the introduction of the concept of squirt flow. A wide range of squirt flow models exist, but the predictions of these models contradict each other and those of poroelasticity. We argue that a valid squirt flow model should be consistent with the evidence in favour of poroelasticity and with the rigorous results of effective medium theory. We then proceed to derive such a model for a simple pore space consisting of a randomly oriented collection of small aspect ratio cracks and spherical pores. However, compliance with our constraints is not a sufficient condition for the model to be a valid representation of rock. We build confidence in the approach by showing that a range of geometries can be handled without complicating the mathematical form of the model. Indeed, the model can be expressed through macroscopic parameters having physical interpretations that are independent of the specific microstructural geometry. We estimate these parameters for a typical sandstone and demonstrate the predictions of the model.

Key words: cracks, permeability, porosity, viscosity, wave propagation.

1 INTRODUCTION

The Biot–Gassmann theory of poroelasticity (Gassmann 1951; Biot 1956) forms the basis of most investigations into wave propagation in fluid-saturated rocks. The fundamental concept of the theory is to model the dynamic interaction between the fluid and solid phases. Important differences between the predictions of the model and conventional elasticity include the introduction of velocity dispersion, attenuation and the existence of a second 'slow' *P* wave. Numerous attempts have been made to extend the model by means of homogenization theory (Thimus *et al.* 1998).

The slow *P* wave was first observed experimentally by Plona (1980) in synthetic sandstone, while Kelder & Smeulders (1997) were the first to observe it in naturally occurring rock. Thomsen (1985) and Bourbie *et al.* (1987) have argued that the confirmation of the existence of this wave suggests the validity of the remainder of Biot's predictions.

In the low-frequency limit, Biot's equations reduce to those of Gassmann (1951). Gassmann's formulae allow the saturated bulk and shear moduli to be calculated from the dry rock moduli, the bulk moduli of the rock mineral and saturating fluid and porosity. The result is given by

$$\kappa_{\rm sat} = \kappa_{\rm dry} + \frac{\left(1 - \kappa_{\rm dry}/\kappa_{\rm m}\right)^2}{\phi/\kappa_{\rm f} + (1-\phi)/\kappa_{\rm m} + \kappa_{\rm dry}\Big/\kappa_{\rm m}^2}, \tag{1}$$

$$\mu_{\rm sat} = \mu_{\rm dry}, \tag{2}$$

where ϕ is the porosity, κ refers to the bulk modulus, μ is the shear modulus, the subscripts sat, dry, m and f refer to the saturated rock, the dry rock, the rock mineral and the saturating fluid, respectively.

Thomsen (1985) and Wang & Nur (1992) present evidence in favour of Gassmann's theorem for a wide range of different rock types. It is noticeable that Gassmann's theorem appears to work well when applied to rocks subjected to high values of effective stress but underestimates the velocity when low values of effective stress are applied.

Conventionally, this discrepancy is considered to be caused by dispersion. Laboratory measurements are typically carried out at high (roughly 1 MHz) frequencies, in contrast to the zero-frequency assumption that underlies Gassmann's prediction. Unfortunately, the magnitude of dispersion predicted by the full dynamic Biot equations is typically too low to account for these measurements (Winkler 1985, 1986; Han

1987; Mochizuki 1982; Wang & Nur 1990). An accurate prediction of the magnitude of dispersion is essential if ultrasonic measurements are to be used in the interpretation of low-frequency seismic data.

A second problem with the Biot–Gassmann predictions concerns the response to changing fluid viscosity. The Biot theory makes the prediction that velocity decreases with increasing fluid viscosity. It is observed experimentally, however, that velocities increase with increasing fluid viscosity (Nur 1980; Jones & Nur 1983; Jones 1986).

The concept of squirt flow (Mavko & Nur 1975) addresses these two concerns simultaneously. Squirt flow models are unanimous in predicting higher values of dispersion than the conventional Biot theory, and they also predict that velocity increases with increasing fluid viscosity.

Squirt flow models differ from the Biot theory in so far as it is assumed that there exist pressure gradients in the fluid that do not point in the direction of wave propagation. Mechanisms that account for this require a degree of heterogeneity in the pore space. It is often argued that a seismic wave compresses compliant cracks more than stiffer pores, with a resulting exchange of fluid, or that flow can take place between cracks of differing orientations. This provides an explanation as to why the squirt flow effect only appears to be prevalent at low effective stresses; at high effective stresses cracks are closed, removing the possibility of squirt flow and Gassmann's formula works well. Models for these effects can be divided into two classes: microscopic and macroscopic.

Macroscopic models do not require any description of the geometry at the pore scale. This is an obvious advantage in that it is not necessary to deal with parameters such as, for example, the crack aspect ratio, which can be hard to define and measure, but this is achieved at the expense of geometrical approximations. It remains an open question to determine any errors introduced by these approximations.

Mavko & Jizba (1991) gave a high-frequency analogue to Gassmann's formula on the basis of a macroscopic squirt flow model. They found that bulk dispersion and shear dispersion were proportional to each other. Dvorkin *et al.* (1995) interpolated between the Gassmann formula and the theory of Mavko & Jizba (1991) to allow velocity and attenuation to be calculated at any frequency. Dvorkin & Nur (1993) attempted to incorporate squirt flow directly into the Biot model (the so-called BISQ model). Unfortunately, this model is not consistent with Gassmann's formula at zero frequency, which led the authors to suggest that it would be more applicable for the case of partial saturation.

Since squirt flow is a consequence of the microscale geometry, it appears natural to attempt to model it with a microstructural model. O'Connell & Budiansky (1977) derived a model in which the details of crack geometry played a dominant role.

O'Connell & Budiansky (1977) assumed that the pore space consisted entirely of an isotropic collection of fluid-saturated cracks of small aspect ratio. When the rock was subjected to bulk compression, the same pressure would then be induced in every crack. Under this assumption they argued that the bulk modulus of the saturated rock would be equal to the bulk modulus of the mineral making up the rock. This contradicts Gassmann's formula.

O'Connell & Budiansky (1977) argue that under shear stress the situation is different. The shear stress will in general induce different pressures in cracks of different orientations, and fluid is expected to flow down these pressure gradients. This situation is modelled with the equation

$$\frac{d\theta}{dt} = \frac{d\tilde{\sigma}}{dt} + \frac{4r^3a^3\tilde{\sigma}}{\eta}, \tag{3}$$

where θ is the dilatation in a crack, $\tilde{\sigma}$ is the normal effective stress acting on the crack under consideration, r is the aspect ratio, a is the crack radius and η is the fluid viscosity.

When this modelling is incorporated into a self-consistent effective medium calculation a characteristic frequency emerges:

$$\omega_1 = \frac{\kappa_m r^3}{\eta}. \tag{4}$$

It is of importance to note that this frequency depends on the cube of the crack aspect ratio. Since one would expect a wide range of different aspect ratios to be present in real rock, a critical issue concerns how the analysis is to be extended to distributions of aspect ratios. O'Connell & Budiansky (1977) state without proof that the characteristic frequencies of each individual crack type can be superposed linearly and independently. This implies that the shape of the dispersion curve depends crucially on the aspect ratio distribution.

Johnston *et al.* (1979) give results similar to O'Connell & Budiansky (1977), but in their model the driving mechanism is flow between thin cracks and spherical pores. Velocities and attenuations are calculated from the model of Kuster & Toksoz (1974), where the fluid bulk modulus is assigned a frequency-dependent imaginary part. They find that the characteristic frequency is proportional to the square of the crack aspect ratio, but they do not consider the case where a range of aspect ratios are present. Their model predicts that when no pores are present there is no dispersion in either the bulk or shear modulus, in direct contradiction to O'Connell & Budiansky (1977) results.

Both O'Connell & Budiansky (1977) and Johnston *et al.* (1979) predict the existence of a 'viscous relaxation' effect owing to shearing of the viscous fluid inside individual cracks. The characteristic frequency for this effect is higher than that for squirt flow, and it is unclear whether this effect can take place at sufficiently low frequencies to be observed, even in ultrasonic tests.

Hudson *et al.* (1996) gave a number of methods for placing fluid flow into the standard Hudson model (Hudson 1980, 1981). In the first model the pore space is assumed to consist entirely of parallel cracks. This is then extended to include distributions of microcracks. The driving mechanisms in the model are the exchange of fluid between cracks of different orientations and flow on a larger spatial scale driven by the pressure gradient induced by the seismic wave. These flow mechanisms are coupled by the introduction of an average pressure field. It is noticeable that when the result for two identical sets of cracks is computed we do not recover the previous result for a single set of parallel

cracks. This matter requires clarification. When the particular case of an isotropic crack distribution is considered Hudson *et al.*'s (1996) results indicate that there is dispersion in the bulk modulus caused by the macroscopic flow and dispersion in the shear modulus.

A weakness of this formulation is that no account is taken of rounder pores. Sedimentary rocks often have porosities of over 20 per cent, of which perhaps not more than 1 per cent can be considered to be caused by microcracks. To model such rocks, Hudson *et al.* (1996) introduce an 'equant porosity' model.

The driving mechanisms of the equant porosity model are exchange of fluid between cracks and spherical pores, and global flow in the direction of wave propagation. No account is taken of exchange of fluid between cracks of different orientations. Formally, the only difference between the equant porosity model and the standard model of Hudson (1981) lies in the crack opening parameter U_{33}, which gives the response of a crack to normal stress. The result is

$$U_{33} = \frac{4}{3}\frac{\lambda_m + 2\mu}{\lambda_m + \mu}(1 + K)^{-1}, \tag{5}$$

where

$$K = \frac{\kappa_f}{\pi \mu r}\frac{\lambda_m + 2\mu}{\lambda_m + \mu}[1 + 3(1 - i)J/2c]^{-1}, \tag{6}$$

$$J^2 = \frac{\phi_m \kappa_f k}{2\omega\eta}, \tag{7}$$

with k being the permeability, λ_m and μ the Lamé parameters, and ϕ_m the porosity associated with the pores. Note that the expression given for J^2 by Hudson *et al.* (1996) was in error. This has been corrected in a subsequent paper (Hudson *et al.* 2001).

When the frequency, ω is equal to zero the result reduces to exactly that given for dry cracks by Hudson (1981). This means that at zero frequency the saturated rock behaves exactly as if it were dry, in contradiction to Gassmann's theorem.

Pointer *et al.* (2000) presented a numerical investigation of the model of Hudson *et al.* (1996) and extended the results to the case of partial saturation. Tod (2001) used this model to consider the case of 'nearly aligned cracks'. In this model the distribution of cracks is similar to the case of a single aligned crack set, but scope exists for squirt flow because of small variations in crack orientation and aspect ratio.

It is clear that substantial contradictions exist between the predictions of the various models. This is partly because the models consider different pore spaces, combinations of cracks and pores as opposed to just collections of cracks, but there also exist disagreements between models that consider the same pore space. It is important to find principles that will resolve these contradictions.

Endres & Knight (1997), in a substantial generalization of the paper by Budiansky & O'Connell (1980), gave rigorous results for calculating the magnitude of dispersion produced by the squirt flow effect for a range of pore space geometries. Their high-frequency elastic moduli are the standard effective medium theory results that assume that no fluid exchange takes place. For the low-frequency moduli they assume perfect fluid pressure communication, allowing the magnitude of dispersion to be calculated by a comparison of low- and high-frequency moduli. They show that their low-frequency results are compatible with Gassmann's theorem.

While the formulae that Endres & Knight (1997) present are valid for distributions of inclusions with any aspect ratio between zero and one, their analysis of the simple case of a collection of spherical pores and cracks of small aspect ratios shows behaviour that is more complicated than that of any of the models studied so far. This shows clearly the limitations of these models.

Endres & Knight (1997) consider the case where the total porosity is fixed, but the geometrical configuration of that porosity is allowed to vary. When the porosity consists entirely of spherical pores, both shear stress and bulk compression induce identical pressures in each pore. There are therefore no pressure gradients in the fluid, which implies that no flow takes place and both the bulk and shear moduli are non-dispersive. At the other extreme, when the pore space consists of an isotropic distribution of cracks flow can take place. Since a shear stress induces different pressures in cracks of different orientations, pressure gradients will exist and this will lead to relieving flow. In this case the shear modulus will be dispersive. Under bulk compression the pressure in each crack will be identical and no flow will take place, leading to a non-dispersive bulk modulus.

Endres & Knight (1997) interpolate between these extremes, calculating bulk and shear dispersion as a function of the fraction of a given porosity, which is composed of cracks. Shear dispersion is seen to be an increasing function of this crack fraction, whereas bulk dispersion, which vanishes when the crack fraction is zero and one, achieves a maximum for a particular intermediate value of the crack fraction.

It is interesting to compare the predictions of the squirt flow models with the results of Endres & Knight (1997). The BISQ model of Dvorkin & Nur (1993) cannot strictly be compared with that of Endres & Knight (1997), since it violates Gassmann's theorem at zero frequency. Dvorkin *et al.* (1995) claim that their model holds for general microgeometry, and so, in particular, it should hold for the case of cracks and spherical pores considered by Endres & Knight (1997). Their model, however, clearly violates the results of Endres & Knight (1997) with its prediction that shear dispersion is simply proportional to bulk dispersion.

A similar objection can be made to the model of Johnston *et al.* (1979). They considered an identical physical problem to Endres & Knight (1997), in which the pore space was assumed to consist of thin ellipsoidal cracks and spherical pores, but they too found that shear dispersion was proportional to bulk dispersion.

O'Connell & Budiansky's (1977) model considers the case where cracks alone are present, and they achieve qualitative agreement with Endres & Knight's (1997) result that for such a pore space there would be dispersion only in the shear modulus. There is no indication, however, of how to extend their results to the case of higher porosities.

A similar conclusion may be drawn with regard to the first, interconnected crack, model of Hudson *et al.* (1996). They considered pore space to consist of cracks alone; however, in this case the bulk modulus is dispersive since account is taken of global flow along pressure gradients induced by the seismic wave. The equant porosity model of Hudson *et al.* (1996) violates Gassmann's formula, so it is not meaningful to compare it with the results of Endres & Knight (1997).

We argue that the contradictions that exist between the predictions of the different squirt flow models can be traced to their failure to be consistent with the results of Endres & Knight (1997). Rocks in the Earth's crust typically have porosities that are too high to be modelled by a collection of thin cracks. A valid squirt flow model has therefore to treat pore spaces, which consist of both thin cracks and rounder pores. The interaction between the cracks and pores should conform to the behaviour described by Endres & Knight (1997), with the exception of the case of global flow on a wavelength scale at high frequency, which was not considered by Endres & Knight (1997).

Our philosophy is that if a squirt flow model is to be considered as an improvement over the standard Biot–Gassmann theory of poroelasticity then it must reproduce the successes of that theory. This implies that it must be compatible with Gassmann's theorem for zero frequency. Thomsen (1985) first suggested that this constraint was appropriate. Given that the slow *P* wave is now commonly observed (Plona 1980; Klimentos & McCann 1988; Kelder & Smeulders 1997) it also seems reasonable to demand that a squirt flow model should be able to predict the existence of this wave.

It is clear that none of the squirt flow models reviewed in this paper satisfy the three constraints that we propose: consistency with Gassmann's formulae, the existence of the Biot wave and consistency with Endres & Knight (1997). In the remainder of this paper we derive a model that does satisfy these constraints.

Unfortunately, the converse to our reasoning is in general false. Even though our proposed model satisfies our constraints, it does not follow that it is a valid representation of rock, nor does it follow that its parametrization is sufficiently amenable to allow predictions to be made and the model tested. The restriction of the model to distributions of cracks all of the same aspect ratio is a drawback, since we expect cracks of all aspect ratios to be present in rock. Many of the parameters that appear in the model are specific to the idealized geometry, and this inhibits the application of the model to studying the behaviour of real rocks. The questions of validity and practicality can only be answered fully by testing the model in detail on laboratory data. In this paper we give a partial answer to these issues.

We show that the model can be extended to cover a range of different crack aspect ratios without complicating its mathematical form. This allows us to treat more realistic pore spaces and increases our confidence in the generality of the approach. Equally importantly, we show that all specifically microstructural parameters can be removed, and the results expressed through macroscopic parameters. Each of these parameters has a well-defined physical interpretation, analogous to an accepted rock property. This gives indications of the parameter values that should be used for modelling purposes.

As a step in the direction of a full laboratory test of the model, we choose parameters to simulate standard rock properties and study the predicted dependence of velocity and attenuation on petrophysical parameters. A crucial parameter is the timescale parameter τ, which determines whether a given frequency should be considered as high, low or intermediate. Since τ has to be considered as an unknown parameter we will present those relationships that involve τ in non-dimensional form. It is straightforward to demonstrate numerically that the model is indeed consistent with the analysis of Endres & Knight (1997).

2 FLUID DYNAMICS FORMULATION

To begin our modelling, we consider rock to consist of a linearly elastic solid permeated with two kinds of voids: uniformly sized and shaped ellipsoidal cracks of small aspect ratio, and uniformly sized spherical pores. We will use the expression 'element of pore space' as a generic term referring to any void, with no implication as to whether it is a crack or a pore. We require that all fluid flow take place between one element of pore space and another. This means that for elements a and b we will write independently of shape and orientation:

$$\partial_t m_a = \frac{\rho_0 k \varsigma}{\eta}(p_b - p_a), \tag{8}$$

where m_a is the mass in element a, ρ_0 is the fluid density, k is the permeability, ς is the grain size and p_a is the fluid pressure in element a. Two length-scales are implicit in this equation: the separation distance between elements and the radius of the surface through which fluid flows. For simplicity we have identified both scales with the grain size, although other choices are possible. We will require eq. (8) to hold equally well if subscripts a and b are interchanged, ensuring the conservation of pore fluid mass.

The purpose of the model is to describe the propagation of plane waves, so we may define a direction that will be taken to be the direction of the propagation of this wave. We let the coordinate x denote the position along this axis of wave propagation. Consider an element of pore space situated at position x on this axis. We imagine that this element exchanges fluid with six other elements of pore space, one situated in front of it with coordinate $x + \varsigma$, one behind it with coordinate $x - \varsigma$ and four with coordinate x. This in effect gives a network model.

We want to imagine elements of pore space placed at random on the vertices of our network, and to this end we must describe the orientations that the cracks may take up. Each possible crack orientation may be represented by a point on the surface of the unit sphere. We now partition the surface of the unit sphere into N_c elements of equal area. We will now let

$$\varpi = \frac{(\phi_c / c_v)}{(\phi_p / p_v)}, \tag{9}$$

where ϕ_c is the fraction of the total volume occupied by cracks and c_v is the volume of an individual crack and similarly for pores. We then define

$$N_p = \frac{N_c}{\varpi} \tag{10}$$

and

$$N = N_c + N_p. \tag{11}$$

Now define a collection of elements C consisting of N_c cracks, each with a different orientation corresponding to one of the elements of the partition, together with N_p pores. At each vertex of the network we will place an element of pore space drawn at random from C.

The expected pressure in the element at any given vertex is now

$$E[p(x)] = \frac{1}{N}\sum_{j=1}^{N_c} E[p_j(x)] + \frac{N_p}{N}E[p^*(x)], \tag{12}$$

where p_j represents the pressure in a crack of orientation j and p^* is the pressure in the pores.

Assuming that the flow law, eq. (8), holds between all adjacent vertices of the network and that these flows may be added linearly, we write:

$$E[\partial_t m_i(x)] = \frac{4\rho_0 k\varsigma}{\eta}\{E[p(x)] - E[p_i(x)]\} + \frac{\rho_0 k\varsigma}{\eta}\{E[p(x+\varsigma)] + E[p(x-\varsigma)] - 2E[p_i(x)]\}. \tag{13}$$

Observing no distinction between values and their expectations, the full system may be written in a convenient matrix form:

$$\begin{bmatrix} \dot m_1 \\ \vdots \\ \dot m_{N_c} \\ \vdots \\ \dot m_N \end{bmatrix} = \frac{4\rho_0 k\varsigma}{\eta N}\begin{bmatrix} (1-N) & 1 & 1 & & 1 \\ 1 & (1-N) & 1 & \cdots & 1 \\ 1 & 1 & (1-N) & & 1 \\ & \vdots & & \ddots & \vdots \\ 1 & 1 & 1 & \cdots & (1-N) \end{bmatrix}\begin{bmatrix} p_1 \\ p_2 \\ p_3 \\ \vdots \\ p^* \end{bmatrix}$$
$$+ \frac{\rho_0 k\varsigma}{\eta N}\begin{bmatrix} 1 & 1 & 1 & & 1 \\ 1 & 1 & 1 & \cdots & 1 \\ 1 & 1 & 1 & & 1 \\ & \vdots & & \ddots & \vdots \\ 1 & 1 & 1 & \cdots & 1 \end{bmatrix}\begin{bmatrix} p_1(x-\varsigma)+p_1(x+\varsigma) \\ p_2(x-\varsigma)+p_2(x+\varsigma) \\ p_3(x-\varsigma)+p_3(x+\varsigma) \\ \vdots \\ p^*(x-\varsigma)+p^*(x+\varsigma) \end{bmatrix} - \frac{2\rho_0 k\varsigma}{\eta}\begin{bmatrix} p_1 \\ p_2 \\ p_3 \\ \vdots \\ p^* \end{bmatrix}. \tag{14}$$

As with all effective medium theories, it is necessary to assume that the wavelength is larger than the grain size. This means that we can write

$$p_i(x-\varsigma) + p_i(x+\varsigma) = 2p_i(x) + \varsigma^2 p_i''(x), \tag{15}$$

whereupon if

$$\bar p = \frac{1}{N}\sum_{i=1}^{N} p_i, \tag{16}$$

the system transforms to

$$\begin{bmatrix} \dot m_1 \\ \dot m_2 \\ \dot m_3 \\ \vdots \\ \dot m_N \end{bmatrix} = \frac{6\rho_0 k\varsigma}{\eta N}\begin{bmatrix} (1-N) & 1 & 1 & & 1 \\ 1 & (1-N) & 1 & \cdots & 1 \\ 1 & 1 & (1-N) & & 1 \\ & \vdots & & \ddots & \vdots \\ 1 & 1 & 1 & \cdots & (1-N) \end{bmatrix}\begin{bmatrix} p_1 \\ p_2 \\ p_3 \\ \vdots \\ p^* \end{bmatrix} + \frac{\rho_0 k\varsigma^3}{\eta}\begin{bmatrix} \bar p'' \\ \bar p'' \\ \bar p'' \\ \vdots \\ \bar p'' \end{bmatrix}. \tag{17}$$

If we now let

$$A = \begin{bmatrix} 1 & 1 & 1 & & 1 \\ 1 & -1 & 0 & \cdots & 0 \\ 1 & 0 & -1 & & 0 \\ & \vdots & & \ddots & \vdots \\ 1 & 0 & 0 & \cdots & -1 \end{bmatrix}, \tag{18}$$

then

$$A\begin{bmatrix}\dot{m}_1\\ \dot{m}_2\\ \dot{m}_3\\ \vdots\\ \dot{m}_N\end{bmatrix}=\frac{6\rho_0 k\varsigma}{\eta}\begin{bmatrix}0&0&0&&0\\0&-1&0&\cdots&0\\0&0&-1&&0\\&\vdots&&\ddots&\vdots\\0&0&0&\cdots&-1\end{bmatrix}A\begin{bmatrix}p_1\\p_2\\p_3\\\vdots\\p^*\end{bmatrix}+\frac{\rho_0 k\varsigma^3}{\eta}A\begin{bmatrix}\bar{p}''\\\bar{p}''\\\bar{p}''\\\vdots\\\bar{p}''\end{bmatrix}. \tag{19}$$

Now if we write

$$\bar{m}=\frac{1}{N}\sum_{i=1}^{N}m_i, \tag{20}$$

then the first row reads as

$$\dot{\bar{m}}=\frac{\rho_0 k\varsigma^3}{\eta}\bar{p}'', \tag{21}$$

and subsequent rows are given by

$$\dot{m}_1-\dot{m}_i=\frac{6\rho_0 k\varsigma}{\eta}(p_i-p_1),\qquad 2\le i\le N. \tag{22}$$

Now the choice of subscript 1 is clearly arbitrary, so in general

$$\dot{m}_i-\dot{m}_j=\frac{6\rho_0 k\varsigma}{\eta}(p_j-p_i),\qquad 1\le i,j\le N. \tag{23}$$

Fixing $j>N_c$ and summing from $i=1,\ldots,N_c$ we find

$$\langle\dot{m}\rangle_c-\dot{m}^*=\frac{6\rho_0 k\varsigma}{\eta}\Big(p^*-\langle p\rangle_c\Big), \tag{24}$$

where

$$\langle p\rangle_c=\frac{1}{N_c}\sum_{i=1}^{N_c}p_i, \tag{25}$$

$$\langle m\rangle_c=\frac{1}{N_c}\sum_{i=1}^{N_c}m_i, \tag{26}$$

and since the conditions in each pore are identical we have introduced the notation m^* for the mass in each pore. Eq. (24) describes the exchange of fluid between the cracks and pores.

We show in the Appendix that the fluid mass in each crack and pore can be written in terms of the applied stress and fluid pressure. Let $c_v$and p_v be the crack and pore volumes, μ the mineral shear modulus, v the Poisson ratio, κ_f the fluid bulk modulus and r the crack aspect ratio. Then, if we introduce the definitions $\sigma_c=\pi\mu r/2(1-v)$, $K_c=\sigma_c/\kappa_f$ and $K_p=4\mu/3\kappa_f$, eqs (A15) and (A16) show that

$$\langle\dot{m}\rangle_c=\frac{c_v\rho_0}{\sigma_c}\left[(1+K_c)\langle\dot{p}\rangle_c-\frac{\dot{\sigma}}{3}\right], \tag{27}$$

$$\dot{m}^*=\frac{3p_v\rho_0}{4\mu}\left[(1+K_p)\dot{p}^*-\frac{1-v}{1+v}\dot{\sigma}\right], \tag{28}$$

provided that the partition of the unit sphere is taken to be sufficiently refined that $\frac{1}{N_c}\sum_{i=1}^{N_c}\sigma_i=\sigma/3$, where σ_i is the normal stress acting on the ith crack and σ is the trace of the applied stress tensor.

Now with the definitions

$$\gamma=\frac{3p_v\sigma_c(1+K_p)}{4c_v\mu(1+K_c)}, \tag{29}$$

$$\gamma'=\gamma\frac{1-v}{1+v}\frac{1}{1+K_p}, \tag{30}$$

$$\frac{1}{\tau}=\frac{6k\varsigma\sigma_c}{\eta c_v(1+K_c)}, \tag{31}$$

eq. (24) may be written as

$$\langle \dot{p} \rangle_c - \gamma \dot{p}^* + \left[\gamma' - \frac{1}{3(1+K_c)} \right] \dot{\sigma} = \frac{1}{\tau} \Big(p^* - \langle p \rangle_c \Big). \tag{32}$$

This expression may be integrated, giving

$$\langle p \rangle_c = \gamma p^* + \left[\frac{1}{3(1+K_c)} - \gamma' \right] \sigma - \frac{1}{\tau} \int_0^t \left\{ (\gamma - 1) p^*(s) + \left[\frac{1}{3(1+K_c)} - \gamma' \right] \sigma(s) \right\} \mathrm{e}^{(s-t)/\tau} \, ds. \tag{33}$$

Arguing directly from (23) with the same logic gives the expression

$$p_i = \frac{\sigma_i}{1+K_c} + \gamma p^* - \gamma' \sigma - \frac{1}{\tau} \int_0^t \left[\frac{\sigma_i(s)}{1+K_c} + (\gamma - 1) p^* - \gamma' \sigma(s) \right] \mathrm{e}^{(s-t)/\tau} \, ds. \tag{34}$$

These expressions are appealing since in the limit $\tau \to 0$:

$$\frac{1}{\tau} \mathrm{e}^{(s-t)/\tau} \to \delta(s-t), \tag{35}$$

where $\delta(s-t)$ is the Dirac delta function, and so

$$p_i \to p^*. \tag{36}$$

This means that in the limit of immediate pressure relaxation, the pressure in each crack is identical and the same as that in the pores, in accordance with Gassmann's theory.

So far we have described how the pressure in each element of the pore space may be given in terms of the two fields, p^* and σ. It is clear that p^* and σ must themselves be coupled. From eqs (16) and (20):

$$\bar{p} = \iota \langle p \rangle_c + (1 - \iota) p^*, \tag{37}$$

$$\bar{m} = \iota \langle m \rangle_c + (1 - \iota) m^*, \tag{38}$$

where

$$\iota = \frac{N_c}{N} \tag{39}$$

and

$$\langle \dot{p} \rangle_c = \gamma \dot{p}^* + \frac{(1-\gamma)}{\tau} p^* + \left[\frac{1}{3(1+K_c)} - \gamma' \right] \left(\dot{\sigma} - \frac{1}{\tau} \sigma \right) + \frac{1}{\tau^2} \int_0^t \left\{ (\gamma - 1) p^*(s) + \left[\frac{1}{3(1+K_c)} - \gamma' \right] \sigma(s) \right\} \mathrm{e}^{(s-t)/\tau} \, ds, \tag{40}$$

$$\langle p \rangle_c'' = \gamma p^{*\prime\prime} + \left[\frac{1}{3(1+K_c)} - \gamma' \right] \sigma'' - \frac{1}{\tau} \int_0^t \left\{ (\gamma - 1) p^{*\prime\prime}(s) + \left[\frac{1}{3(1+K_c)} - \gamma' \right] \sigma''(s) \right\} \mathrm{e}^{(s-t)/\tau} \, ds. \tag{41}$$

We can write eq. (21) as

$$\begin{aligned} &\frac{\iota}{\tau}(1-\gamma) p^* + \gamma \dot{p}^* - \frac{\iota}{\tau} \left[\frac{1}{3(1+K_c)} - \gamma' \right] \sigma - \gamma' \dot{\sigma} + \frac{\iota}{\tau^2} \int_0^t \left\{ (\gamma - 1) p^*(s) + \left[\frac{1}{3(1+K_c)} - \gamma' \right] \sigma(s) \right\} \mathrm{e}^{(s-t)/\tau} \, ds \\ &\quad = \frac{\varsigma^2}{6\tau} [\iota\gamma + (1-\iota)] p^{*\prime\prime} + \frac{\varsigma^2 \iota}{6\tau} \left[\frac{1}{3(1+K_c)} - \gamma' \right] \sigma'' - \frac{\varsigma^2 \iota}{6\tau^2} \int_0^t \left\{ (\gamma - 1) p''(s) + \left[\frac{1}{3(1+K_c)} - \gamma' \right] \sigma''(s) \right\} \mathrm{e}^{(s-t)/\tau} \, ds. \end{aligned} \tag{42}$$

This may be reduced to the differential equation:

$$\gamma \ddot{p}^* + \frac{1}{\tau} [\iota + (1-\iota)\gamma] \dot{p}^* - \frac{\varsigma^2}{6\tau} [1 - \iota(1-\gamma)] \dot{p}^{*\prime\prime} - \frac{\varsigma^2}{6\tau^2} p^{*\prime\prime} = \gamma' \ddot{\sigma} + \frac{1}{\tau} \left[\frac{\iota}{3(1+K_c)} + (1-\iota)\gamma' \right] \dot{\sigma} + \frac{\varsigma^2 \iota}{6\tau} \left[\frac{1}{3(1+K_c)} - \gamma' \right] \dot{\sigma}''. \tag{43}$$

This equation gives the required coupling between the fields p^* and σ. Taking the Fourier transform ($\tilde{f} = \int_{-\infty}^{\infty} \int_{-\infty}^{\infty} f(x,t) \, \mathrm{e}^{-i(lx+\omega t)} \, dx \, dt$) of eq. (43) gives the expression

$$\begin{aligned} &\left\{ -(\omega\tau)^2 \gamma + i(\omega\tau)[\iota + \gamma(1-\iota)] + \frac{i}{6}(\varsigma l)^2 (\omega\tau)[1 - \iota(1-\gamma)] + \frac{1}{6}(\varsigma l)^2 \right\} \tilde{p} \\ &= \left\{ -(\omega\tau)^2 \gamma' + i(\omega\tau) \left[\frac{\iota}{3(1+K_c)} + (1-\iota)\gamma' \right] - \frac{i}{6}(\varsigma l)^2 (\omega\tau) \left[\frac{\iota}{3(1+K_c)} - \iota\gamma' \right] \right\} \tilde{\sigma}, \end{aligned} \tag{44}$$

where l is the wavenumber.

3 THE P-WAVE DISPERSION EQUATION

To find the dispersion relation for the propagation of P waves it is necessary to derive a second equation between p^* and σ. This second equation arises out of a generalization of Eshelby's approach to finding the effective elastic constants of a solid permeated with inclusions. Eshelby's (1957) interaction energy formula, reviewed in the Appendix, eq. (A19), for the effective elastic tensor gives an expression for the effective P-wave modulus $M_{\rm eff}$:

$$M_{\rm eff} = M - \frac{1}{s^2}\sum_t \phi_t\left(\sigma_{ij}^{\rm w}\epsilon_{ij}^{\rm inc} - \sigma_{ij}^{\rm inc}\epsilon_{ij}^{\rm w}\right), \tag{45}$$

where the superscript 'w' refers to the field of the travelling wave, the superscript 'inc' refers to the field in the inclusion and $s = \epsilon_{11}^{\rm w}$. In the classical approach to the problem $\epsilon^{\rm inc}$ would be calculated using the Wu T tensor (Wu 1966):

$$\epsilon^{\rm inc} = T\epsilon^{\rm w}, \tag{46}$$

and then $\sigma^{\rm inc}$ would follow from

$$\sigma^{\rm inc} = C^{\rm inc}\epsilon^{\rm inc}. \tag{47}$$

These values would be inserted directly into eq. (45) to give an effective P-wave modulus as a function of the geometry and elastic constants of the inclusions.

In our case, however, the state of stress and strain in the fluid-saturated inclusion depends on the details of the fluid dynamics. Under the assumption of a zero fluid shear modulus, $\epsilon^{\rm inc}$ and $\sigma^{\rm inc}$ can be calculated from eq. (34) and the formula of Zatsepin & Crampin (1997), discussed in the Appendix (eq. A6):

$$\epsilon^{\rm inc} = (I - S)^{-1}C^{-1}(\sigma^{\rm w} - CSC^{-1}p\delta). \tag{48}$$

To achieve consistency with the approach of Walsh (1969) we will calculate the off-diagonal terms of $\sigma^{\rm inc}$ and $\epsilon^{\rm inc}$ using the Wu T tensor under the assumption that the fluid shear modulus is $i\omega\eta$. The result of this calculation is given in eq. (A3).

In this way, our effective elastic tensor will depend on both σ and p^*, and the general wave equation:

$$\rho\ddot{u}_i = \sigma_{ij,j}, \tag{49}$$

where ρ is the density of the saturated rock, will give nothing more than an equation coupling σ and p^*. In eq. (49), and in the remainder of this paper, we assume the summation convention. This will be the second equation that we need for the derivation of the dispersion relationship.

To carry out this process explicitly, we first need to ensure that all of our tensors are expressed in the same coordinate system. In classical elasticity the stress and strain tensors associated with the propagation of a P wave are given by

$$\sigma^{\rm w} = \frac{\sigma(t)}{3\kappa_{\rm m}}\begin{bmatrix}\lambda_{\rm m}+2\mu & 0 & 0\\ 0 & \lambda_{\rm m} & 0\\ 0 & 0 & \lambda_{\rm m}\end{bmatrix}, \tag{50}$$

$$\epsilon^{\rm w} = \frac{\sigma(t)}{3\kappa_{\rm m}}\begin{bmatrix}1 & 0 & 0\\ 0 & 0 & 0\\ 0 & 0 & 0\end{bmatrix}, \tag{51}$$

where $\lambda_{\rm m}$ and μ are the matrix Lamé constants. We now rotate these tensors into the frame of a crack the normal of which (x_1, say) has Euler angles (ψ, θ), and find that the relevant terms are

$$\sigma^{\rm wloc} = \frac{\sigma(t)}{3\kappa_{\rm m}}\begin{bmatrix}\lambda_{\rm m}+2\mu\cos^2\psi & 0 & -2\mu\sin\psi\cos\psi\\ 0 & \lambda_{\rm m} & 0\\ -2\mu\sin\psi\cos\psi & 0 & \lambda_{\rm m}+2\mu\sin^2\psi\end{bmatrix}, \tag{52}$$

$$\epsilon^{\rm wloc} = \frac{\sigma(t)}{3\kappa_{\rm m}}\begin{bmatrix}\cos^2\psi & 0 & -\sin\psi\cos\psi\\ 0 & 0 & 0\\ -\sin\psi\cos\psi & 0 & \sin^2\psi\end{bmatrix}, \tag{53}$$

where the notation 'loc' is introduced to signify that the tensor has been rotated into the local frame of the crack.

The tensors $\epsilon^{\rm inc}$ and $\sigma^{\rm inc}$ are given by

$$\epsilon^{\rm inc} = \begin{bmatrix}[\sigma_{11}^{\rm wloc} - p(\psi,\theta)]/\sigma_{\rm c} & T^s\epsilon_{12}^{\rm wloc} & T^s\epsilon_{13}^{\rm wloc}\\ T^s\epsilon_{21}^{\rm wloc} & 0 & 0\\ T^s\epsilon_{31}^{\rm wloc} & 0 & 0\end{bmatrix}, \tag{54}$$

$$\sigma^{\rm inc} = \begin{bmatrix} p(\psi,\theta) & 2i\omega\eta T^s \epsilon_{12}^{\rm wloc} & 2i\omega\eta T^s \epsilon_{13}^{\rm wloc} \\ 2i\omega\eta T^s \epsilon_{21}^{\rm wloc} & p(\psi,\theta) & 0 \\ 2i\omega\eta T^s \epsilon_{31}^{\rm wloc} & 0 & p(\psi,\theta) \end{bmatrix}, \tag{55}$$

where it is shown in eq. (A4) that

$$T^s = \frac{2\mu/(\mu - i\omega\eta)}{i\omega\eta/(\mu - i\omega\eta) + [(2-v)/(1-v)](\pi/2)r}. \tag{56}$$

Eqs (34) and (52) give the expression

$$p(\psi,\theta) = \frac{\sigma(t)}{3\kappa_{\rm m}} \frac{\lambda_{\rm m} + 2\mu\cos^2\psi}{1+K_{\rm c}} + \gamma p^* - \gamma'\sigma(t) - \frac{1}{\tau}\int_0^t \left[\frac{\sigma(s)}{3\kappa_{\rm m}} \frac{\lambda_{\rm m} + 2\mu\cos^2\psi}{1+K_{\rm c}} + (\gamma-1)p^*(s) - \gamma'\sigma(s)\right] {\rm e}^{(s-t)/\tau}\, ds, \tag{57}$$

so that

$$\begin{aligned} \epsilon_{ij}^{\rm inc}\sigma_{ij}^{\rm w} = \frac{\sigma(t)}{3\kappa_{\rm m}} \Bigg\{ & \frac{K_{\rm c}\left(\lambda_{\rm m} + 2\mu\cos^2\psi\right)^2}{3\kappa_{\rm m}\sigma_{\rm c}(1+K_{\rm c})}\sigma(t) - \frac{\gamma\left(\lambda_{\rm m} + 2\mu\cos^2\psi\right)}{\sigma_{\rm c}} p^*(t) + \frac{\gamma'\left(\lambda_{\rm m} + 2\mu\cos^2\psi\right)}{\sigma_{\rm c}}\sigma(t) \\ & + \frac{1}{\tau}\int_0^t \left[\frac{\left(\lambda_{\rm m} + 2\mu\cos^2\psi\right)^2}{3\kappa_{\rm m}\sigma_{\rm c}(1+K_{\rm c})}\sigma(s) + \frac{(\gamma-1)\left(\lambda_{\rm m} + 2\mu\cos^2\psi\right)}{\sigma_{\rm c}} p^*(s) - \frac{\gamma'\left(\lambda_{\rm m} + 2\mu\cos^2\psi\right)}{\sigma_{\rm c}}\sigma(s)\right] \\ & \times {\rm e}^{(s-t)/\tau}\, ds + 4\mu T^s \sin^2\psi\cos^2\psi \frac{\sigma(t)}{3\kappa_{\rm m}} \Bigg\}. \end{aligned} \tag{58}$$

We now integrate this expression over orientation, $d\Omega$, to obtain

$$\begin{aligned} \epsilon_{ij}^{\rm inc}\sigma_{ij}^{\rm wloc} = \frac{\sigma(t)}{3\kappa_{\rm m}} \Bigg(& \left[\frac{K_{\rm c}L_2}{3\kappa_{\rm m}\sigma_{\rm c}(1+K_{\rm c})} + \frac{\gamma' L_1}{\sigma_{\rm c}} + \frac{8}{45}\frac{\mu}{\kappa_{\rm m}} T^s\right]\sigma(t) - \frac{\gamma L_1}{\sigma_{\rm c}} p^*(t) \\ & + \frac{1}{\tau}\int_0^t \left\{\left[\frac{L_2}{3\kappa_{\rm m}\sigma_{\rm c}(1+K_{\rm c})} - \frac{\gamma' L_1}{\sigma_{\rm c}}\right]\sigma(s) + \frac{(\gamma-1)L_1}{\sigma_{\rm c}} p^*(s)\right\} {\rm e}^{(s-t)/\tau}\, ds \Bigg), \end{aligned} \tag{59}$$

where we have introduced the notation

$$L_1 = \lambda_{\rm m} + \tfrac{2}{3}\mu, \tag{60}$$

$$L_2 = \lambda_{\rm m}^2 + \tfrac{4}{3}\lambda_{\rm m}\mu + \tfrac{4}{5}\mu^2. \tag{61}$$

By similar means it may be shown that

$$\sigma_{ij}^{\rm inc}\epsilon_{ij}^{\rm wloc} = \frac{\sigma(t)}{3\kappa_{\rm m}} \left(\left[\frac{L_1}{3\kappa_{\rm m}(1+K_{\rm c})} - \gamma' - \frac{8}{15} i\omega\eta T^s \frac{1}{\kappa_{\rm m}}\right]\sigma(t) + \gamma p^*(t) - \frac{1}{\tau}\int_0^t \left\{\left[\frac{L_1}{3\kappa_{\rm m}(1+K_{\rm c})} - \gamma'\right]\sigma(s) + (\gamma-1)p^*(s)\right\} {\rm e}^{(s-t)/\tau}\, ds \right), \tag{62}$$

so we may write

$$\sum^{\rm cracks} \phi_i(\epsilon^{\rm inc}\sigma^{\rm w} - \epsilon^{\rm w}\sigma^{\rm inc}) = \frac{\phi_{\rm c}\sigma(t)}{3\kappa_{\rm m}} \left\{ d_1\sigma(t) + d_2 p^*(t) + \frac{1}{\tau}\int_0^t \left[d_3\sigma(s) + d_4 p^*(s)\right] {\rm e}^{(s-t)/\tau}\, ds \right\}, \tag{63}$$

where

$$\mathcal{M} = \frac{2\mu}{i\omega\eta/(\mu - i\omega\eta) + [(2-v)/(1-v)]\,(\pi/2)r}, \tag{64}$$

$$d_1 = \frac{K_{\rm c}L_2}{3\kappa_{\rm m}\sigma_{\rm c}(1+K_{\rm c})} + \frac{\gamma' L_1}{\sigma_{\rm c}} - \frac{L_1}{3\kappa_{\rm m}(1+K_{\rm c})} + \gamma' + \frac{8}{45\kappa_{\rm m}}\mathcal{M}, \tag{65}$$

$$d_2 = -\gamma\left(\frac{L_1}{\sigma_{\rm c}} + 1\right), \tag{66}$$

$$d_3 = \frac{L_2}{3\kappa_{\rm m}\sigma_{\rm c}(1+K_{\rm c})} - \frac{\gamma' L_1}{\sigma_{\rm c}} + \frac{L_1}{3\kappa_{\rm m}(1+K_{\rm c})} - \gamma', \tag{67}$$

$$d_4 = (\gamma - 1)\left(\frac{L_1}{\sigma_c} + 1\right) \tag{68}$$

and ϕ_c is the porosity associated with the cracks.

We now perform the same calculations for pores. Applying eq. (48) we find:

$$\epsilon_{11}^{inc} = \frac{3}{4\mu}\frac{1-v}{1+v}\left(\lambda_m + 2\mu\frac{9+5v}{7-5v}\right)\frac{\sigma(t)}{3\kappa_m} - \frac{p^*(t)}{4\mu}, \tag{69}$$

$$\epsilon_{22}^{inc} = \epsilon_{33}^{inc} = \frac{3}{4\mu}\frac{1-v}{1+v}\left(\lambda_m - 2\mu\frac{1+5v}{7-5v}\right)\frac{\sigma(t)}{3\kappa_m} - \frac{p^*(t)}{4\mu}. \tag{70}$$

Eqs (50) and (51) now give:

$$\epsilon_{ij}^{inc}\sigma_{ij}^{w} = \frac{\sigma(t)}{3\kappa_m}\left\{\frac{3}{4\mu}\frac{1-v}{1+v}\left[\left(\lambda_m + 2\mu\frac{9+5v}{7-5v}\right)(\lambda_m + 2\mu) + 2\lambda_m\left(\lambda_m - 2\mu\frac{1+5v}{7-5v}\right)\right]\frac{\sigma(t)}{3\kappa_m} - \frac{3\kappa_m}{4\mu}p^*\right\}, \tag{71}$$

$$\sigma_{ij}^{inc}\epsilon_{ij}^{w} = \frac{\sigma(t)}{3\kappa_m}p^*(t), \tag{72}$$

so that we may write

$$\sum^{pores}\phi_i(\epsilon^{inc}\sigma^{w} - \sigma^{inc}\epsilon^{w}) = \phi_p\frac{\sigma(t)}{3\kappa_m}\Big[d_5\sigma(t) - d_6p^*\Big], \tag{73}$$

where

$$d_5 = \frac{1}{4\kappa_m\mu}\frac{1-v}{1+v}\left[\left(\lambda_m + 2\mu\frac{9+5v}{7-5v}\right)(\lambda_m + 2\mu) + 2\lambda_m\left(\lambda_m - 2\mu\frac{1+5v}{7-5v}\right)\right], \tag{74}$$

$$d_6 = \frac{3}{4}\frac{\kappa_m}{\mu} + 1, \tag{75}$$

and ϕ_p is the porosity associated with the spherical pores.

Eq. (45) now gives:

$$M_{eff}\sigma(x,t) = M\sigma(x,t) - 3\phi_c\kappa_m\left\{d_1\sigma(x,t) + d_2p^*(x,t) + \frac{1}{\tau}\int_0^t\Big[d_3\sigma(x,s) + d_4p^*(x,s)\Big]e^{(s-t)/\tau}\,ds\right\} - 3\phi_p\kappa_m\Big[d_5\sigma(x,t) - d_6p^*(x,t)\Big]. \tag{76}$$

By analogy with the analysis of Biot (1956), we will seek solutions of the form:

$$p^* = F_1\exp i(lx - \omega t), \tag{77}$$

$$\sigma = F_2\exp i(lx - \omega t). \tag{78}$$

If we now multiply eq. (76) by $\exp(-ilx)$ we see that M_{eff} must be independent of x. This means that we can differentiate (45) to arrive at

$$M_{eff}\sigma'' = M\sigma'' - 3\phi_c\kappa_m\left\{d_1\sigma'' + d_2p^{*\prime\prime} + \frac{1}{\tau}\int_0^t\Big[d_3\sigma''(s) + d_4p^{*\prime\prime}(s)\Big]e^{(s-t)/\tau}\,ds\right\} - 3\phi_p\kappa_m\Big(d_5\sigma'' - d_6p^{*\prime}\Big). \tag{79}$$

If we take the Fourier transform of this equation we obtain

$$F(M_{eff}\sigma'') = -l^2M\tilde{\sigma} + l^2 3\phi_c\kappa_m\left[d_1\tilde{\sigma} + d_2\tilde{p} + \frac{1}{1+i\omega\tau}(d_3\tilde{\sigma} + d_4\tilde{p})\right] + l^2 3\phi_p\kappa_m(d_5\tilde{\sigma} - d_6\tilde{p}). \tag{80}$$

However, the equation of motion in effective medium theory is given by

$$\rho\ddot{\sigma} = M_{eff}\sigma'', \tag{81}$$

so taking the Fourier transform we find

$$-\rho\omega^2\tilde{\sigma} = -l^2M\tilde{\sigma} + l^2 3\phi_c\kappa_m\left[d_1\tilde{\sigma} + d_2\tilde{p} + \frac{1}{1+i\omega\tau}(d_3\tilde{\sigma} + d_4\tilde{p})\right] + l^2\phi_p 3\kappa_m[d_5\tilde{\sigma} - d_6\tilde{p}], \tag{82}$$

which may be rewritten as

$$\left[(l^2M-\rho\omega^2)-\phi_c l^2 3\kappa_m\left(d_1+\frac{d_3}{1+i\omega\tau}\right)-\phi_p l^2 d_5\right]\tilde{\sigma}-\left[l^2\phi_c\kappa_m\left(d_2+\frac{d_4}{1+i\omega\tau}\right)-l^2 3\kappa_m\phi_p d_6\right]\tilde{p}=0. \tag{83}$$

If we write eq. (83) as

$$\left(A_1+A_2l^2\right)\tilde{\sigma}+\left(A_3+A_4l^2\right)\tilde{p}=0, \tag{84}$$

and eq. (44) as

$$\left(B_1+B_2l^2\right)\tilde{\sigma}+\left(B_3+B_4l^2\right)\tilde{p}=0, \tag{85}$$

then the dispersion equation of the system is given by

$$\begin{vmatrix} A_1+A_2l^2 & A_3+A_4l^2 \\ B_1+B_2l^2 & B_3+B_4l^2 \end{vmatrix}=0. \tag{86}$$

Note that this equation is quadratic in l^2, so the model predicts the existence of two compressional wave velocities, in agreement with Biot's theory of poroelasticity. Frequency-dependent *P*-wave velocities can be calculated directly from eq. (86).

4 THE *S*-WAVE DISPERSION EQUATION

The situation with shear waves is less complicated. Eq. (A19) gives

$$\mu_{\rm eff}=\mu-\frac{\mu^2}{[\sigma(t)]^2}\sum\phi_i(\sigma^{\rm w}\epsilon^{\rm inc}-\sigma^{\rm inc}\epsilon^{\rm w}), \tag{87}$$

where the stress tensor associated with the propagation of a shear wave is given by

$$\sigma^{\rm w}=\begin{bmatrix} 0 & 0 & \sigma(t) \\ 0 & 0 & 0 \\ \sigma(t) & 0 & 0 \end{bmatrix}. \tag{88}$$

When this tensor is rotated into the frame of a crack the normal of which has Euler angles (ψ,θ) we find

$$\sigma^{\rm wloc}=\sigma(t)\begin{bmatrix} 2\sin\psi\cos\psi\cos\theta & \cos\psi\sin\theta & \cos\theta(\cos^2\psi-\sin^2\psi) \\ \cos\psi\sin\theta & 0 & -\sin\psi\sin\theta \\ \cos\theta(\cos^2\psi-\sin^2\psi) & -\sin\psi\sin\theta & -2\sin\psi\cos\psi\cos\theta \end{bmatrix}. \tag{89}$$

The strains are given by

$$\epsilon^{\rm w}=\frac{1}{2\mu}\sigma^{\rm w}, \tag{90}$$

$$\epsilon^{\rm wloc}=\frac{1}{2\mu}\sigma^{\rm wloc}, \tag{91}$$

The stress and strain in a crack of orientation (ψ,θ) are:

$$\sigma^{\rm inc}=\begin{bmatrix} p(\psi,\theta) & 2i\omega\eta T^s\epsilon_{12}^{\rm wloc} & 2i\omega\eta T^s\epsilon_{13}^{\rm wloc} \\ 2i\omega\eta T^s\epsilon_{21}^{\rm wloc} & p(\psi,\theta) & 0 \\ 2i\omega\eta T^s\epsilon_{31}^{\rm wloc} & 0 & p(\psi,\theta) \end{bmatrix}, \tag{92}$$

$$\epsilon^{\rm inc}=\begin{bmatrix} [\sigma_{11}^{\rm wloc}-p(\psi,\theta)]/\sigma_c & T^s\epsilon_{12}^{\rm wloc} & T^s\epsilon_{13}^{\rm wloc} \\ T^s\epsilon_{21}^{\rm wloc} & 0 & 0 \\ T^s\epsilon_{31}^{\rm wloc} & 0 & 0 \end{bmatrix}, \tag{93}$$

where eq. (34) now gives

$$p(\psi,\theta)=\frac{2\sin\psi\cos\psi\cos\theta\sigma(t)}{1+K_c}-\frac{1}{\tau}\int_0^t\frac{2\sin\psi\cos\psi\cos\theta\sigma(s)}{1+K_c}{\rm e}^{(s-t)/\tau}\,ds. \tag{94}$$

For cracks, we then find

$$\sigma_{ij}^{\mathrm{w}}\epsilon_{ij}^{\mathrm{inc}} - \sigma_{ij}^{\mathrm{inc}}\epsilon_{ij}^{\mathrm{w}} = 4\sin^2\psi\cos^2\psi\cos^2\theta\frac{\sigma(t)}{\sigma_{\mathrm{c}}}\left[\frac{K_{\mathrm{c}}}{1+K_{\mathrm{c}}}\sigma(t) + \frac{1}{\tau}\int_0^t \frac{\sigma(s)}{1+K_{\mathrm{c}}}\mathrm{e}^{(s-t)/\tau}\,ds\right]$$
$$+\left[\frac{\sigma(t)}{\mu}\right]^2[\cos^2\psi\sin^2\theta + \cos^2\theta(\cos^2\psi - \sin^2\psi)^2]\mathcal{M}. \tag{95}$$

Integrating over $d\Omega$ gives

$$\sum^{\mathrm{cracks}}\phi_t\left(\sigma_{ij}^{\mathrm{wloc}}\epsilon_{ij}^{\mathrm{inc}} - \epsilon_{ij}^{\mathrm{wloc}}\sigma_{ij}^{\mathrm{inc}}\right) = \frac{4}{15}\frac{\sigma(t)}{\sigma_{\mathrm{c}}}\left[\frac{K_{\mathrm{c}}}{1+K_{\mathrm{c}}}\sigma(t) + \frac{1}{\tau}\int_0^t\frac{\sigma(s)}{1+K_{\mathrm{c}}}\mathrm{e}^{(s-t)/\tau}\right] + \frac{2}{5}\left\{\frac{\sigma(t)}{\mu}\right\}^2\mathcal{M}. \tag{96}$$

For pores from eq. (48)

$$\epsilon^{\mathrm{inc}} = \frac{15}{2\mu}\frac{1-v}{7-5v}\sigma(t)\begin{bmatrix}0&0&1\\0&0&0\\1&0&0\end{bmatrix}, \tag{97}$$

where we have neglected terms of order $i\omega\eta/\mu$ and therefore

$$\sigma^{\mathrm{inc}} = 0, \tag{98}$$

and so

$$\sum^{\mathrm{pores}}\phi_i\left(\sigma_{ij}^{\mathrm{w}}\epsilon_{ij}^{\mathrm{inc}} - \sigma_{ij}^{\mathrm{inc}}\epsilon_{ij}^{\mathrm{w}}\right) = \phi_{\mathrm{p}}\frac{15}{\mu}\frac{1-v}{7-5v}[\sigma(t)]^2. \tag{99}$$

Substituting these results into eq. (87) we find

$$\mu_{\mathrm{eff}}\sigma = \mu\sigma - \frac{4}{15}\phi_{\mathrm{c}}\frac{1}{1+K_{\mathrm{c}}}\frac{\mu^2}{\sigma_{\mathrm{c}}}\left[K_{\mathrm{c}}\sigma + \frac{1}{\tau}\int_0^t\sigma(s)\mathrm{e}^{(s-t)/\tau}\,ds\right] - \frac{2}{5}\phi_{\mathrm{c}}\mathcal{M}\sigma - 15\phi_{\mathrm{p}}\frac{1-v}{7-5v}\mu\sigma. \tag{100}$$

Noting once again that μ_{eff} is independent of x, we may differentiate twice with respect to x to obtain

$$\mu_{\mathrm{eff}}\sigma'' = \mu\sigma'' - \frac{4}{15}\phi_{\mathrm{c}}\frac{1}{1+K_{\mathrm{c}}}\frac{\mu^2}{\sigma_{\mathrm{c}}}\left[K_{\mathrm{c}}\sigma'' + \frac{1}{\tau}\int_0^t\sigma''(s)\mathrm{e}^{(s-t)/\tau}ds\right] - \frac{2}{5}\phi_{\mathrm{c}}\mathcal{M}\sigma'' - 15\phi_{\mathrm{p}}\frac{1-v}{7-5v}\mu\sigma''. \tag{101}$$

The equation of motion is

$$\rho\ddot{\sigma} = \mu_{\mathrm{eff}}\sigma'', \tag{102}$$

so taking the Fourier transform and dividing by $\tilde{\sigma}$ we obtain the dispersion equation:

$$\rho\omega^2 = l^2\left[\mu - \frac{4}{15}\phi_{\mathrm{c}}\frac{1}{1+K_{\mathrm{c}}}\frac{\mu^2}{\sigma_{\mathrm{c}}}\left(K_{\mathrm{c}} + \frac{1}{1+i\omega\tau}\right) - \phi_{\mathrm{c}}\frac{2}{5}\mathcal{M} - 15\phi_{\mathrm{p}}\mu\frac{1-v}{7-5v}\right]. \tag{103}$$

Eq. (103) permits the explicit computation of frequency-dependent *S*-wave velocities.

5 RECOVERY OF GASSMANN'S THEOREM

Thomsen (1985) notes that the conditions on which Gassmann's theorem is based are very general, and he argues convincingly that any theory that makes stronger assumptions than Gassmann, such as the model just derived, should nevertheless reproduce Gassmann's theorem when its conditions are satisfied. Endres & Knight (1997) prove the Gassmann consistency of Eshelby's interaction energy method when pore pressure equalization is allowed for, but show that neither the self-consistent scheme nor the differential effective medium approximation give a Gassmann-consistent result. We now show that our model is Gassmann consistent in the zero-frequency limit.

The case of the shear modulus is straightforward. Considering the Fourier transform of eq. (100) and dividing by $\tilde{\sigma}$ we find

$$\mu_{\mathrm{eff}} = \mu - \frac{4}{15}\phi_{\mathrm{c}}\frac{1}{1+K_{\mathrm{c}}}\frac{\mu^2}{\sigma_{\mathrm{c}}}\left(K_{\mathrm{c}} + \frac{1}{1+i\omega\tau}\right) - \frac{2}{5}\phi_{\mathrm{c}}\mathcal{M} - 15\phi_{\mathrm{p}}\mu\frac{1-v}{7-5v}. \tag{104}$$

We note that the fluid properties appear in three variables: τ, K_{c} and $\mathcal{M}$. In the expression $\mathcal{M}$, the fluid viscosity appears multiplied by frequency, ω. This means that when $\omega = 0$, $\mathcal{M}$ will be independent of viscosity and fluid type. Similarly, τ is multiplied by ω and so this dependence on fluid properties disappears in the zero-frequency limit. When the term in τ disappears, however, the terms in $(1 + K_{\mathrm{c}})$ cancel out, and the whole expression is therefore independent of fluid type. Explicitly, when $\omega = 0$ we have

$$\mu_{\rm eff} = \mu - \frac{4}{15}\phi_{\rm c}\frac{\mu^2}{\sigma_{\rm c}} - \frac{8}{5}\phi_{\rm c}\frac{(1-v)\mu}{(2-v)\pi r} - 15\phi_{\rm p}\mu\frac{1-v}{7-5v}, \tag{105}$$

and it is clear that there is no dependence on fluid properties in this equation. This verifies Gassmann's theorem for the shear modulus.

We will now derive the dry frame bulk modulus. We consider rock subjected to a constant stress field:

$$\sigma^{\rm w} = \sigma\begin{bmatrix}1 & 0 & 0\\ 0 & 1 & 0\\ 0 & 0 & 1\end{bmatrix}. \tag{106}$$

The expression for the effective bulk modulus is then, from eq. (A19):

$$\kappa_{\rm eff} = \kappa_{\rm m} - \frac{\kappa_{\rm m}^2}{\sigma^2}\sum_t \phi_t\left(\sigma_{ij}^{\rm w}\epsilon_{ij}^{\rm inc} - \sigma_{ij}^{\rm inc}\epsilon_{ij}^{\rm w}\right). \tag{107}$$

For dry conditions we naturally have

$$\sigma^{\rm inc} = 0, \tag{108}$$

and so,

$$\kappa_{\rm dry} = \kappa_{\rm m} - \kappa_{\rm m}^2\left(\frac{9}{4\mu}\frac{1-v}{1+v}\phi_{\rm p} + \frac{\phi_{\rm c}}{\sigma_{\rm c}}\right). \tag{109}$$

For the saturated case, we first assume that at zero frequency the wavelength is sufficiently long that we do not have to consider spatial variations in the stress field. Indeed, Gassmann's theorem also relies on this assumption. This means that we may ignore spatial derivatives and eq. (17) becomes

$$\begin{bmatrix}\dot m_1\\ \dot m_2\\ \dot m_3\\ \vdots\\ \dot m^*\end{bmatrix} = \frac{6\rho_0 k\varsigma}{\eta N}\begin{bmatrix}1-N & 1 & 1 & & 1\\ 1 & 1-N & 1 & \cdots & 1\\ 1 & 1 & 1-N & & 1\\ & \vdots & & \ddots & \vdots\\ 1 & 1 & 1 & \cdots & 1-N\end{bmatrix}\begin{bmatrix}p_1\\ p_2\\ p_3\\ \vdots\\ p^*\end{bmatrix}. \tag{110}$$

In the static limit $\dot m_i = 0$ and since the square matrix in eq. (21) has nullity 1 we have

$$p_1 = p_2 = \cdots = p^*. \tag{111}$$

We denote this common pressure simply by p. Now eq. (21) gives

$$\left(\phi_{\rm p}\frac{9}{4\mu}\frac{1-v}{1+v} + \frac{\phi_{\rm c}}{\sigma_{\rm c}}\right)\sigma = \left[\phi_{\rm p}\frac{3}{4\mu}(1+K_{\rm p}) + \frac{\phi_{\rm c}}{\sigma_{\rm c}}(1+K_{\rm c})\right]p, \tag{112}$$

or alternatively

$$p = \frac{\phi_{\rm p}(9/4\mu)\left[(1-v)/(1+v)\right] + \phi_{\rm c}/\sigma_{\rm c}}{\phi_{\rm p}(3/4\mu) + \phi_{\rm c}/\sigma_{\rm c} + \phi/\kappa_{\rm f}}\sigma, \tag{113}$$

where we have introduced the notation $\phi = \phi_{\rm c} + \phi_{\rm p}$. Eq. (107) now gives

$$\kappa_{\rm sat} = \kappa_{\rm m} - \kappa_{\rm m}^2\left(\frac{9}{4\mu}\frac{1-v}{1+v}\phi_{\rm p} + \frac{\phi_{\rm c}}{\sigma_{\rm c}}\right) + \frac{\kappa_{\rm m}^2 p}{\sigma}\left(\frac{\phi_{\rm c}}{\sigma_{\rm c}} + \frac{3}{4\mu}\phi_{\rm p} + \frac{\phi}{\kappa_{\rm m}}\right), \tag{114}$$

which may be written with eqs (109) and (113) as

$$\kappa_{\rm sat} = \kappa_{\rm dry} + \frac{\kappa_{\rm m}\left[\phi_{\rm c}/\sigma_{\rm c} + (3/4\mu)\phi_{\rm p} + \phi/\kappa_{\rm m}\right]\left\{(9/4\mu)[(1-v)/(1+v)]\phi_{\rm p} + \phi_{\rm c}/\sigma_{\rm c}\right\}}{(3/4\mu)\phi_{\rm p} + \phi_{\rm c}/\sigma_{\rm c} + \phi/\kappa_{\rm f}}. \tag{115}$$

At this point a complication arises. The derivation of the model so far has been based on eq. (A10):

$$c_v = c_v^0\left(1 - \frac{\sigma_{\rm n}}{\sigma_{\rm c}} + \frac{p}{\sigma_{\rm c}}\right). \tag{116}$$

In fact, the exact expression is (A7)

$$c_v = c_v^0\left(1 - \frac{\sigma_{\rm n}}{\sigma_{\rm c}} - \frac{\sigma_{ll}}{3\kappa_{\rm m}} + \frac{p}{\sigma_{\rm c}}\right), \tag{117}$$

where, following Zatsepin & Crampin (1997), we neglected the term in $1/\kappa_m$ in favour of the terms in $1/\sigma_c$ which are $O(1/r)$. To prove Gassmann's theorem explicitly we need to use the exact expression. We do not believe that it is worthwhile to complicate the derivation of the model by including a term that is negligible, so at this point we will just note that we may equally well write eq. (115) to the same accuracy as

$$\kappa_{sat} = \kappa_{dry} + \frac{\kappa_m \left[\phi_c/\sigma_c + (3/4\mu)\phi_p + \phi_p/\kappa_m\right]\left\{(9/4\mu)[(1-v)/(1+v)]\phi_p + \phi_c/\sigma_c\right\}}{(3/4\mu)\phi_p + \phi_c/\sigma_c - \phi_c/\kappa_m + \phi/\kappa_f}. \tag{118}$$

We now note that

$$\frac{3}{4\mu}\phi_p = \frac{9}{4\mu}\frac{1-v}{1+v}\phi_p - \frac{\phi_p}{\kappa_m}, \tag{119}$$

and by eq. (109)

$$\frac{9}{4\mu}\frac{1-v}{1+v}\phi_p + \frac{\phi_c}{\sigma_c} = \frac{1}{\kappa_m} - \frac{\kappa_{dry}}{\kappa_m^2}, \tag{120}$$

so that eq. (118) may be written as

$$\kappa_{sat} = \kappa_{dry} + \frac{\left(1 - \kappa_{dry}/\kappa_m\right)^2}{(1-\phi)/\kappa_m + \phi/\kappa_f - \kappa_{dry}\Big/\kappa_m^2}. \tag{121}$$

This is Gassmann's theorem.

6 EXTENSION OF THE ANALYSIS TO DISTRIBUTIONS OF CRACK ASPECT RATIOS

In the analysis of O'Connell & Budiansky (1977) there associated with each crack was a critical frequency proportional to the cube of the crack aspect ratio, and the shape of the dispersion curve predicted by the model therefore depended on the distribution of crack aspect ratios. The analysis presented so far relies on a more detailed description of the fluid dynamics than does O'Connell & Budiansky (1977), and leads to a different conclusion.

The timescale parameter τ in the model was given by (31):

$$\tau = \frac{\eta c_v (1 + K_c)}{6k\varsigma\sigma_c}, \tag{122}$$

where η is the fluid viscosity, c_v is the volume of a crack, k is the permeability, ς is the grain size and σ_c and K_c are parameters defined in (A9) and (A18), respectively. We have from (A9):

$$\sigma_c = \frac{\pi\mu r}{2(1-v)}, \tag{123}$$

with μ being the shear modulus, r the aspect ratio and v the Poisson ratio. The crack volume, c_v, is given by

$$c_v = \tfrac{4}{3}\pi a^3 r, \tag{124}$$

where a is the crack radius. It therefore follows that the aspect ratio terms in eq. (122) will cancel out. The aspect ratio then only appears in eq. (122), through its presence in the term K_c, which is given by eq. (A18)

$$K_c = \frac{\pi}{2(1-v)}\mu c_f r, \tag{125}$$

with c_f being the fluid compressibility, or reciprocal of the fluid bulk modulus. In general, we will not know the value of τ exactly, instead we will be interested only in order of magnitude accuracy. The aspect ratio will only therefore influence τ significantly if $(1 + K_c)$ is of the order of 10. Since the term μc_f will generally be around 20 for water-saturated rock, we can ignore the effect of K_c if $r < 10^{-2}$, when τ will be given by

$$\tau = \frac{4\eta a^3(1-v)}{9k\varsigma\mu}, \tag{126}$$

where there is no dependence on aspect ratio whatsoever. This means that the pressure in a crack is independent of the aspect ratio, and we can consider cracks with distributed aspect ratios without having to modify the calculations for the pressure in each crack as a function of its orientation.

There is still a dependence on the cube of the crack radius, and this might be expected to lead to a distribution of different τ values for cracks of different sizes. This may be correct, but we note that the cracks being of the same size was an important assumption underlying the derivation of the fluid dynamics model. In the analysis we assumed that each crack was connected to six other elements of pore space. If the cracks had been of different sizes then the larger cracks would have to be connected to more elements than would smaller cracks. It is not at all clear how this situation should be modelled, but we could plausibly scale the number of connections with the cube of the crack radius, in which case one would again have a single τ value for each crack. We will accept the assumption that cracks are uniformly sized; Biot (1956)

made a similar assumption and the assumption is implicit in the single characteristic squirt flow length in the BISQ approach (Dvorkin & Nur 1993). Cracks in rock are not uniformly sized, although when plotted by volume, particle size distributions are often very peaked at a characteristic grain size (Mair *et al.* 2000). We believe it is fair to say that the assumption of uniformly sized cracks is less restrictive than the assumption of uniformly shaped cracks.

The only remaining dependence on the aspect ratio is in the parameters $\mathcal{M}$ and d_1 to d_4, eqs (64)(– 68). Terms d_1 to d_4 are $O(1/r)$. When they enter the dispersion equation they are multiplied by ϕ_c, given by

$$\phi_c = \frac{4}{3}\pi\frac{Na^3r}{V} = \frac{4}{3}\pi\epsilon r, \tag{127}$$

where N is the number of cracks in a volume V and ϵ is the crack density. This means that the products $\phi_c d_i$ may be written in the form

$$\phi_c d_i = C\epsilon + C_1 O(\phi_c), \tag{128}$$

where C and C_1 are independent of the aspect ratio. This is essentially the logic behind the statement that the crack density is the appropriate parameter in which to express the effect of cracks on the elasticity of rock (Hudson 1980, 1981) without having to make reference to the aspect ratio spectrum (Murphy 1985).

The situation with the term $\mathcal{M}$ is more subtle. Considering the expression for $\mathcal{M}$:

$$\mathcal{M} = \frac{2\mu}{i\omega\eta/(\mu - i\omega\eta) + [(2-v)/(1-v)](\pi/2)r}, \tag{129}$$

we see that at low frequencies that the term in the aspect ratio will dominate the term in viscosity and $\mathcal{M}$ will essentially be frequency independent. $\mathcal{M}$ will then be $O(1/r)$, and the previous argument will apply once again, giving a dependence on crack density rather than the aspect ratio. When the frequency increases to a point where $\omega\eta/\mu$ is greater than $1/r$, the term in the aspect ratio is dominated by the frequency-dependent viscous term. This effect, leading to velocity dispersion and attenuation, has been studied by Walsh (1969). The frequency at which the effect becomes apparent is controlled by the aspect ratio, and this leads directly to a situation where the shape of the dispersion curve is determined by the aspect ratio spectrum. Nevertheless, for this effect to occur at frequencies of less than 10 MHz the crack aspect ratio has to be extremely low.

We have carried out extensive numerical experiments into the effect of changing the aspect ratio in the model, whilst keeping the crack density constant. For reasonable values of the other parameters there is an almost complete independence of the aspect ratio in the frequency range 0–1 MHz for aspect ratios between $\sim 10^{-2}$ and 10^{-5}. For aspect ratios larger than 10^{-2} the $O(\phi_c)$ terms can sometimes have an effect, while for aspect ratios smaller than 10^{-5} the Walsh effect can be noticeable.

In view of this fact we will assume that all crack aspect ratios are in the band in which crack density alone is important. The input into the model will be crack density. For computational purposes we then choose the aspect ratio arbitrarily to be 10^{-3} and convert the crack density to ϕ_c using eq. (127).

7 ESTIMATION OF PARAMETERS

Perhaps the greatest impediment to the application of microstructural velocity models to the analysis of laboratory data lies in the number of parameters that have to be specified. Many parameters that have a well-defined meaning in the theoretical modelling, for example the crack aspect ratio, cannot be measured directly and therefore become adjustable parameters, greatly reducing the predictive power of the theory. It is therefore imperative to apply the utmost effort to the reduction of the number of adjustable parameters.

Certain of the parameters in the theory can be measured by standard laboratory techniques; these are the porosity, permeability and density of the rock sample together with the fluid properties: fluid density, compressibility and viscosity. The grain size can be estimated with reasonable precision from SEM photographs.

The situation with the elastic tensor is more subtle. In principle, one ought to use the elastic tensor of the mineral that makes up the rock. This can usually be measured directly, but two problems arise immediately. The first difficulty is for samples with complex mineralogy where the use of any one mineral elastic tensor would be inappropriate. A second problem affects rocks with high porosity; the modelling presented so far is limited to dilute concentrations of pores. If it were to be applied to a sandstone of high porosity then the velocity predictions would be expected to be rather poor. If the purpose of the model were to describe the dependence of velocity on mineralogy and porosity (as was the case, for example, in Hornby *et al.* (1994)) we would have to use methods such as the self-consistent scheme (Hill 1965) or the differential effective medium model (Norris 1985) to attempt to account for the elastic interactions. If, however, our interest lies in the variation of a given velocity with frequency, effective stress and pore fluid type then it is possible simply to choose the reference elastic moduli to give reasonable agreement with representative velocities in the rock under consideration. Without this assumption it would not be possible to apply the model to rocks of high porosity.

The parameter γ cannot be measured explicitly nor calculated rigorously from parameters that can be measured. Nevertheless, to prevent it becoming a further adjustable parameter and to ensure as far as possible that reasonable values are taken, we propose an approximation for calculating γ. From eq. (29):

$$\gamma = \frac{3p_v\sigma_c(1+K_p)}{4c_v\mu(1+K_c)}. \tag{130}$$

Since the crack aspect ratios are assumed to be small we take, once again, $K_c = 0$. For cracks and pores of radius a, $p_v = \frac{4}{3}\pi a^3$ and $c_v = \frac{4}{3}\pi a^3 r$. The expression then reduces to

$$\gamma = \frac{3\pi}{8(1-v)}(1 + K_p). \tag{131}$$

An estimate of the Poisson ratio, v, can be made from P and S velocities of the rock, reducing the problem to the estimation of K_p. From eq. (A13)

$$K_p = \frac{4}{3}\frac{\mu}{\kappa_f}. \tag{132}$$

Since μ is a fitted parameter it is best not to use it in this estimation. Instead, we write

$$K_p = \frac{4}{3}\frac{\rho_s}{\rho_f}\left(\frac{V_s}{V_f}\right)^2, \tag{133}$$

where ρ_s and ρ_f are the densities of the saturated solid and fluid, respectively; V_s is a representative shear velocity of the saturated solid and V_f is the acoustic velocity in the fluid. This permits estimation of γ, and an estimate of γ' follows immediately from eq. (30).

The hardest parameter to estimate by ad hoc means is the timescale parameter τ. This parameter is also extremely important, since it will give, in effect, the frequency range over which Gassmann's theorem is valid. Determining appropriate values of τ is an important problem. In this paper we will take τ to be unknown and give relationships that depend on τ in non-dimensional form. The dependence of permeability on effective stress (King *et al.* 1994) suggests the possibility that τ will depend on the effective stress. If measurements of the relationship between permeability and effective stress are available then it is straightforward to introduce this concept into the model.

As it stands, the model does not take account of variations in effective stress. Nur (1971) demonstrated that the imposition of external stress on the rock led to the differential opening and closing of microcracks, modifying the elastic properties of the rock. We may incorporate this effect by including a relationship between the crack density and the effective stress. A number of choices for the functional form are possible, but since the elastic properties of dry rock often have an exponential dependence on external stress (Zhang & Bentley 2000) we propose to use the formula:

$$\epsilon = \epsilon_0 \exp(-c_{cr}\sigma_{eff}), \tag{134}$$

where ϵ_0 and c_{cr} are constants, and σ_{eff} is the effective stress. It should be emphasized that other functional forms for this relationship are possible; dry rock velocities, where they are available, can guide the choice.

The final approximation concerns the relative crack density ι. This was the probability that any element of pore space chosen at random would be a crack, defined in eq. (39) as

$$\iota = \frac{N_c}{N}. \tag{135}$$

Consider a section of rock with volume V. Making the assumption of a single crack and pore radius, a, once again we have

$$\phi_c = \frac{N_c \frac{4}{3}\pi a^3 r}{V} \tag{136}$$

$$\phi_p = \frac{N_p \frac{4}{3}\pi a^3}{V}. \tag{137}$$

Since $N = N_c + N_p$, we have

$$\iota = \frac{\phi_c/r}{\phi_c/r + \phi_p}, \tag{138}$$

or in terms of the crack densities,

$$\iota = \frac{\frac{4}{3}\pi\epsilon}{\frac{4}{3}\pi\epsilon + \phi_p}. \tag{139}$$

As soon as the crack density parameters ϵ_0 and c_{cr} are specified we may use eq. (139) to calculate ι for any value of effective stress.

8 CHOICE OF PARAMETERS AND NUMERICAL RESULTS

The purpose of this section is to choose a set of parameters to illustrate the predictions of the model. This choice is necessarily arbitrary. However, Mavko *et al.* (1998) gave properties of an 'average' water-saturated sandstone under high (30–40 MPa) effective stress. These were a P-wave velocity of 4090 m s^{-1}, an S-wave velocity of 2410 m s^{-1}, a porosity of 16 per cent and a density of 2370 kg m^{-3}.

Using these measurements as a rough guide, we begin to estimate our parameters. We adopt the porosity value of 16 per cent and a density of 2370 kg m^{-3} from the measurements. The grain size is assumed to be 200 μm.

Appropriate values of γ and γ' can be estimated directly. We first estimate K_p from eq. (133), assuming that the acoustic velocity in water is 1500 m s^{-1}:

$$K_p = \frac{4}{3}\frac{\rho_s}{\rho_f}\left(\frac{V_s}{V_f}\right)^2 = \frac{4}{3}(2.37)\left(\frac{2410}{1500}\right)^2 \approx 8. \tag{140}$$

Calculating the Poisson ratio, v, to be 0.24, γ follows from (131) as

$$\gamma = \frac{3\pi}{8(1-v)}(1+K_p) \approx 14. \tag{141}$$

An estimation of γ' follows as

$$\gamma' = \gamma\frac{1-v}{1+v}\frac{1}{1+K_p} \approx 1. \tag{142}$$

We now specify the relationship between the crack density and the effective stress. The crack density has been measured by the inversion of dry velocities (Murphy 1985), the analysis of thin sections (Peacock *et al.* 1994) and observations of shear wave splitting (Crampin 1994). We propose that the relationship

$$\epsilon = 0.3\exp(-0.05\sigma_{\text{eff}}), \tag{143}$$

where σ_{eff} is the effective stress (MPa), is representative.

With these parameters fixed, we now seek reference moduli λ_m and μ, which will give our desired P and S velocities under 40 MPa effective stress at laboratory frequencies, under the assumption that $\omega\tau \gg 1$. We find that $\lambda_m = 1.4 \times 10^{10}$ Pa and $\mu = 2.1 \times 10^{10}$ are satisfactory.

For the frequencies of interest (those less than 10 MHz) we find that the velocities of the fast P and S wave depend on frequency only through the non-dimensional combination $\omega\tau$. In Figs 1 and 2 we plot the relationship between the velocity of P and S waves, respectively, and $\omega\tau$ for a range of effective stresses. Velocities are seen to increase with $\omega\tau$. As the effective stress decreases and more cracks open, there is a drop in the velocity at each frequency and an increase in the dispersion between low- and high-frequency velocities. The attenuation associated with this dispersion is demonstrated in Figs 3 and 4.

The highest values of dispersion occur at low effective stress, when the crack density is at its highest. It should be emphasized that the magnitude of dispersion is sensitive to ϵ_0, while the variation with effective stress is sensitive to c_{cr}. Measured ultrasonic velocities of different types of rock typically show a range of stress sensitivities, and we expect dispersion and attenuation to vary correspondingly.

Since τ depends on viscosity and permeability, there is an implied relationship between the velocity and these variables. To demonstrate this relationship, let η_0 and k_0 be a reference viscosity and permeability, and let τ_0 be the timescale parameter corresponding to these values. In Figs 5 and 6 we show the dependence of the P and S velocity, respectively, on the non-dimensional viscosity, (η/η_0), for two values of $\omega\tau_0$. Velocity increases with viscosity, with the majority of the increase taking place over a viscosity range that is determined by the wave frequency. Figs 7 and 8 repeat the analysis in terms of the non-dimensional permeability (k/k_0). In this case the velocities decrease with increasing permeability.

Unlike the fast P wave, the Biot wave velocity depends jointly on the frequency and the non-dimensional frequency. This situation is illustrated in Fig. 9. Significant Biot wave velocities only occur when the frequency is high and the non-dimensional frequency $\omega\tau$ is low. This requires low values of τ, corresponding, for example, to rocks of very high permeability. The Biot wave is strongly attenuated.

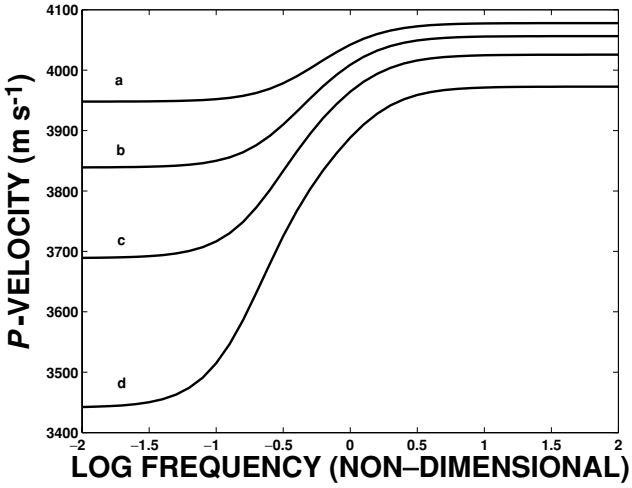

Figure 1. P-wave velocity as a function of $\log(\omega\tau)$ for effective stresses of: (a) 40 MPa, (b) 30 MPa, (c) 20 MPa and (d) 10 MPa.

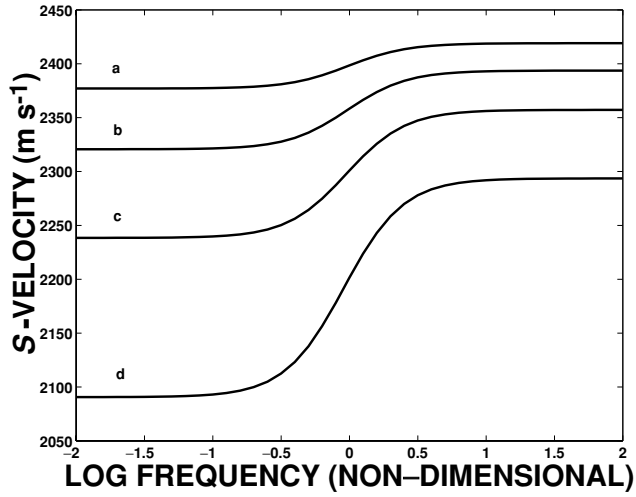

Figure 2. *S*-wave velocity as a function of $\log(\omega\tau)$ for effective stresses of: (a) 40 MPa, (b) 30 MPa, (c) 20 MPa and (d) 10 MPa.

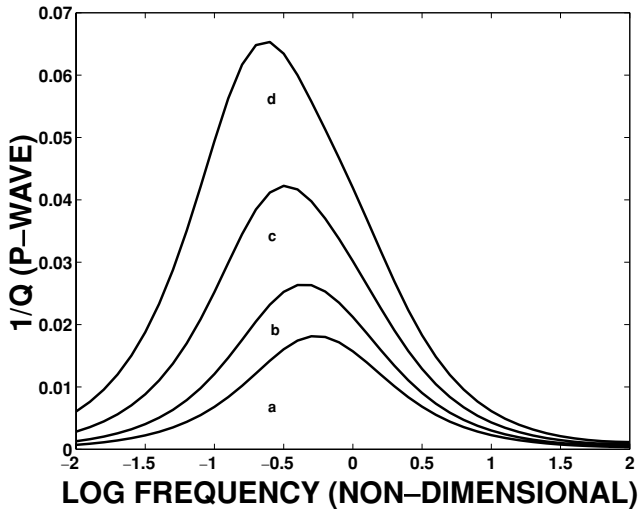

Figure 3. *P*-wave attenuation as a function of $\log(\omega\tau)$ for effective stresses of: (a) 40 MPa, (b) 30 MPa, (c) 20 MPa and (d) 10 MPa.

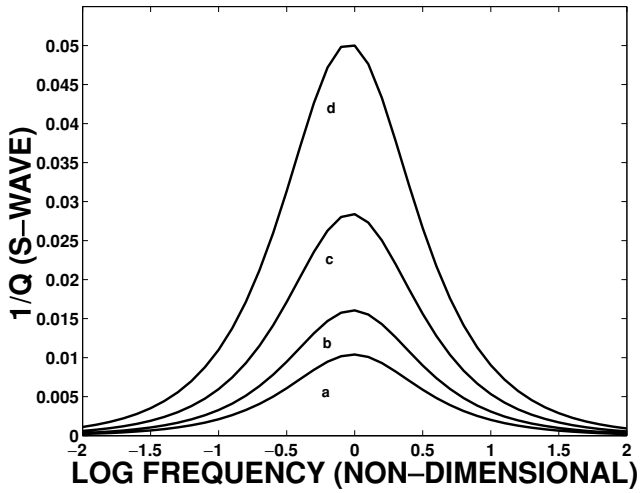

Figure 4. *S*-wave attenuation as a function of $\log(\omega\tau)$ for effective stresses of: (a) 40 MPa, (b) 30 MPa, (c) 20 MPa and (d) 10 MPa.

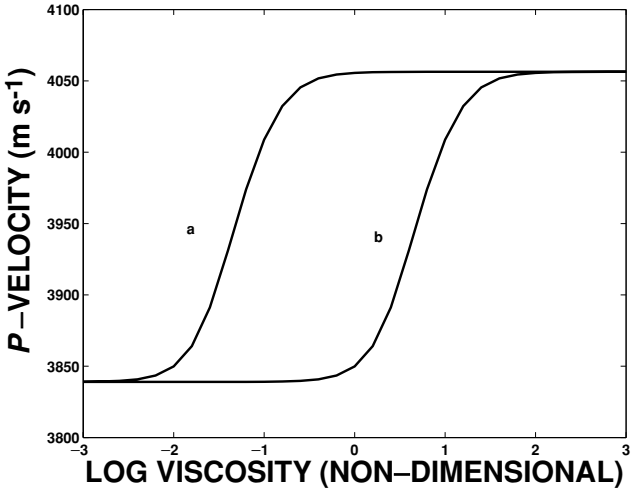

Figure 5. *P*-wave velocity as a function of $\log(\eta/\eta_0)$ for frequencies of: (a) $\omega\tau_0 = 10$ and (b) $\omega\tau_0 = 0.1$ under 30 MPa effective stress.

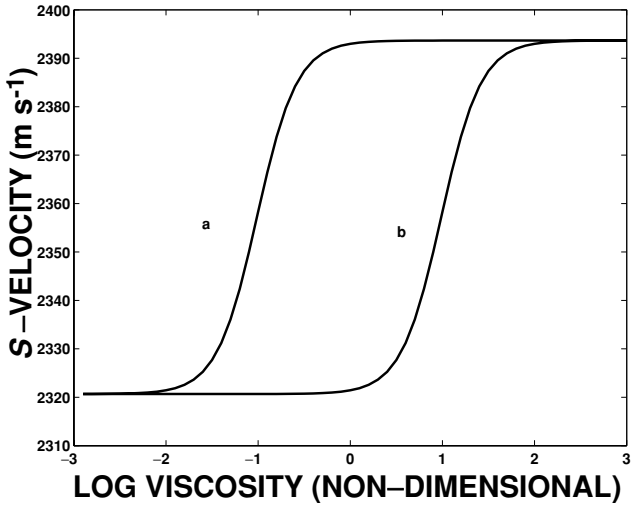

Figure 6. *S*-wave velocity as a function of $\log(\eta/\eta_0)$ for frequencies of: (a) $\omega\tau_0 = 10$ and (b) $\omega\tau_0 = 0.1$ under 30 MPa effective stress.

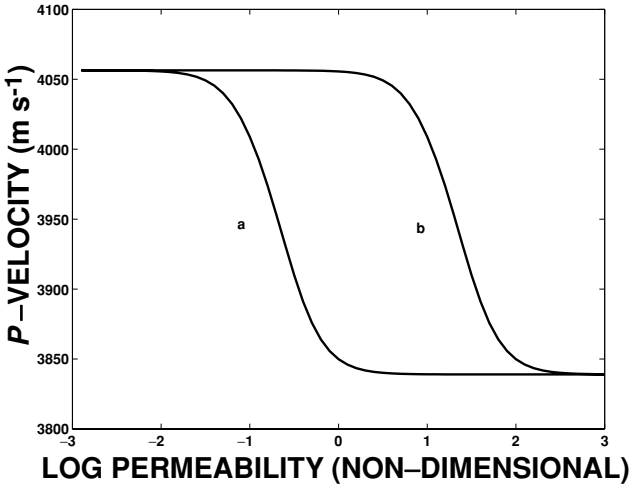

Figure 7. *P*-wave velocity as a function of $\log(k/k_0)$ for frequencies of: (a) $\omega\tau_0 = 0.1$ and (b) $\omega\tau_0 = 10$ under 30 MPa effective stress.

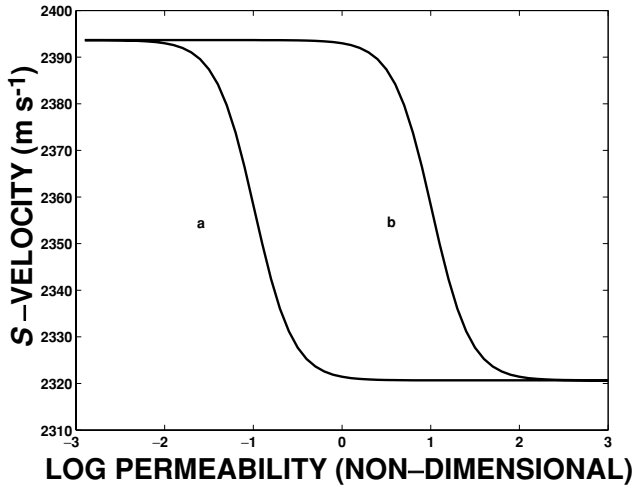

Figure 8. *S*-wave velocity as a function of $\log(k/k_0)$ for frequencies of: (a) $\omega\tau_0 = 0.1$ and (b) $\omega\tau_0 = 10$ under 30 MPa effective stress.

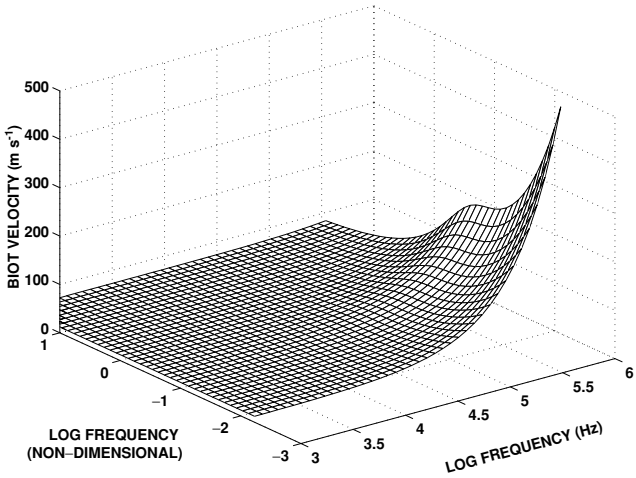

Figure 9. Biot wave velocity as a function of frequency and non-dimensional frequency ($\omega\tau$).

9 COMPARISON WITH THE ANALYSIS OF ENDRES & KNIGHT (1997)

We have argued that consistency with the results of Endres & Knight (1997) is a key requirement for the model. Endres & Knight (1997) considered the case in which porosity consisted of spherical pores and cracks of small aspect ratio. The total porosity was held constant, but the percentage of the porosity that consisted of cracks was allowed to vary from 0 to 100 per cent. The dispersion, defined to be the difference between the low-frequency Gassmann and high-frequency effective medium theory predictions for the bulk and shear modulus, was calculated for each case. The dispersion in the shear modulus was a strictly increasing function of the crack fraction, but the bulk dispersion was zero for the case of 0 and 100 per cent cracks, with a maximum value between these extremes.

We now demonstrate that our model is consistent with these results. We take the total porosity $\phi = \phi_c + \phi_p$ to be 0.1 per cent and calculate the difference in the bulk and shear moduli between non-dimensional frequencies ($\omega\tau$) of 10^{-3} and 10^3. Results as a function of the crack fraction (ϕ_c/ϕ) are plotted in Figs 10 and 11. We find that the possibility of macroscopic flow, which was not considered by Endres & Knight (1997), can be removed by taking ω to be small, ensuring a long wavelength. Note that this crack fraction is not the same as the parameter ι. It can be seen that the behaviour is as described by Endres & Knight (1997).

In this example the shear dispersion was much larger than the bulk dispersion, and this might suggest that bulk dispersion could, in general, be ignored. This is not the case. The magnitude of bulk dispersion is sensitive to the total porosity. Small bulk dispersion values were observed because the total porosity used was small ($\phi = 10^{-3}$).

This effect is illustrated in Fig. 12. We plot the *P*- and *S*-wave dispersion, the difference in m s^{-1} between the low- and high-frequency limits, for a range of different porosities, under 20 MPa effective stress. *S*-wave dispersion is not sensitive to porosity. This is because there is no net flow of fluid between the cracks and the spherical pores. For *P*-wave propagation, however, flow between the cracks and the pores is an important mechanism. Increasing porosity gives a greater scope for this effect to occur, leading to higher values for *P*-wave dispersion for

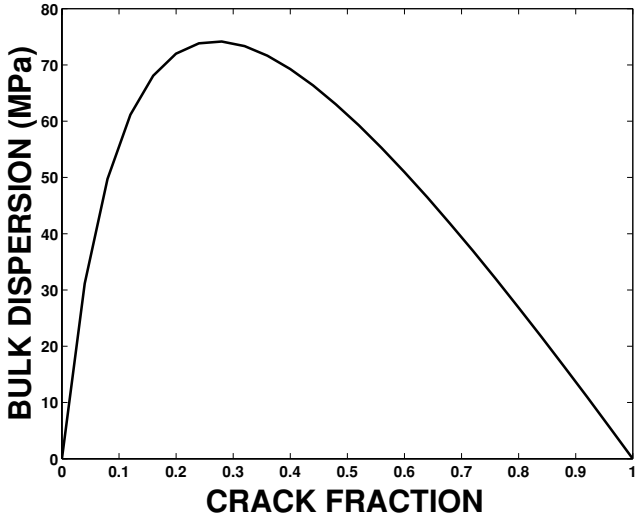

Figure 10. Dispersion in the bulk modulus as a function of the fraction of total porosity occupied by the cracks $[\phi_c/(\phi_c + \phi_p)]$. The total porosity $\phi_c + \phi_p$ is held constant at 0.1 per cent.

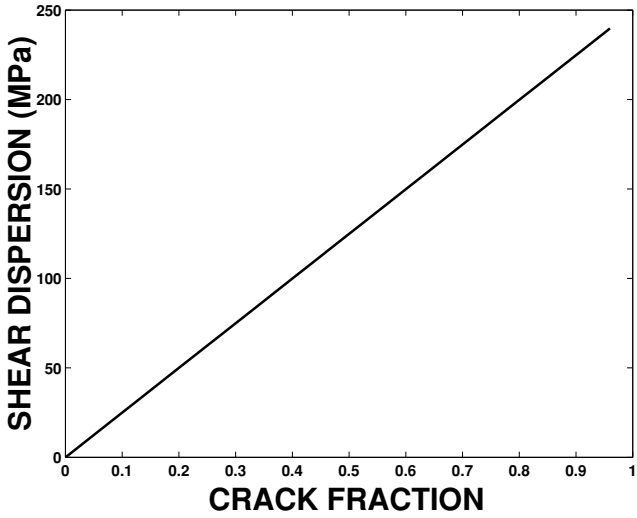

Figure 11. Dispersion in the shear modulus as a function of the fraction of total porosity occupied by the cracks $[\phi_c/(\phi_c + \phi_p)]$. The total porosity $\phi_c + \phi_p$ is held constant at 0.1 per cent.

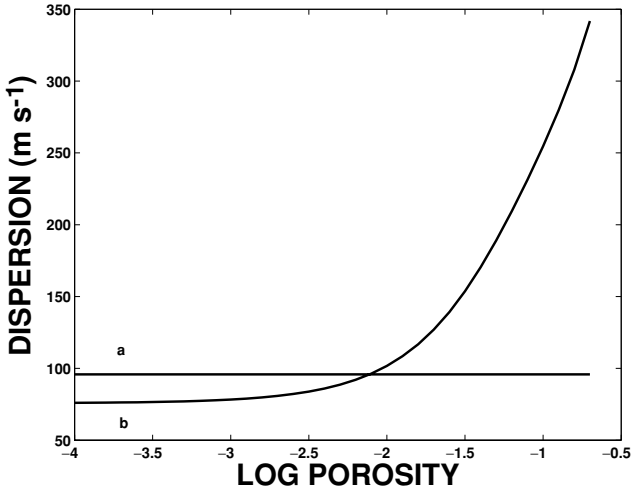

Figure 12. Magnitude of dispersion for (a) *S* wave and (b) *P* wave as a function of porosity associated with spherical pores, ϕ_p. The crack density is held constant at 0.11, corresponding in our model to an effective stress of 20 MPa.

larger porosities. It should be noted that the model of O'Connell & Budiansky (1977) and the connected cracks model of Hudson *et al.* (1996), which model cracks independently of porosity are in effect assuming behaviour that is consistent with the low-porosity limit in Fig. 12. The predicted behaviour of a rock with a porosity of 10 per cent is clearly different from this limit. This shows the importance of incorporating porosity into the model.

10 CONCLUSIONS

A number of different squirt flow models have been proposed previously, principally to address perceived failings in the Biot–Gassmann theory of poroelasticity. While the predictions of these models with regard to the effect of fluid viscosity and the magnitude of dispersion appear to be more in line with the evidence than the Biot theory, they fail to reproduce the major successes of that theory. There is only limited agreement between the predictions of the various models.

We have proposed three principles that a squirt flow model should adhere to. We agree with Thomsen (1985) who argued that such models should reproduce Gassmann's formula at zero frequency. Additionally, however, we believe that it should be possible to demonstrate the existence of the slow *P* wave within the theoretical framework. The contradictions between the individual squirt flow models are to be resolved by insisting that the model should conform to the logic of Endres & Knight (1997), with the only exception being caused by the possible existence of macroscopic flow at high frequencies.

We present the derivation of a squirt flow model in which microstructure is assumed to consist of thin cracks and spherical pores. We show that the model is consistent with the Gassmann formulae at zero frequency and predicts the existence of the slow *P* wave. Qualitative agreement exists with the analysis of Endres & Knight (1997).

We express the model through a macroscopic parametrization. The parameters that appear in the model all have a physical interpretation that corresponds to a well-defined rock property. With the exception of the relaxation time parameter τ, all the parameters can be measured or estimated from measurements. There is no dependence on parameters specific to the idealized geometry from which the model was derived.

A pressure dependence can be introduced with a relationship between crack density and effective stress. The form of the relationship is empirical, and strictly is separate from the derivation of the model. Nevertheless, the predicted dependence of the velocity dispersion and the attenuation on the effective stress is striking. The model predicts that there is potentially a strong dependence of seismic properties on frequency, pressure, viscosity and permeability. This gives rise to a range of potential applications in fields such as the interpretation of time-lapse seismic surveys, pore pressure prediction and the frequency scaling of laboratory measurements.

ACKNOWLEDGMENTS

Mark Chapman was supported through this research firstly by a NERC research studentship and latterly through the NERC thematic programme 'Understanding the micro-to-macro behaviour of rock fluid systems' contract no GST022305. The work is presented with the approval of the Director of the British Geological Survey. Stuart Crampin was partially supported by the EC, contract no EVR1-CT1999-40002. We acknowledge constructive reviews from C. M. van der Kolk and M. Prasad.

REFERENCES

Biot, M.A., 1956. Theory of propagation of elastic waves in a fluid-saturated porous solid. I Low frequency range. II. Higher frequency range, *J. acoust. Soc. Am.,* **28,** 168–191.

Bourbie, T., Coussy, O. & Zinszner, B., 1987. *Acoustics of Porous Media* Gulf Publishing Company, Houston, TX.

Budiansky, B. & O'Connell, R.J., 1980. Bulk dissipation in heterogeneous media, *Solid Earth Geophys. Geotech.,* **42,** 1–10.

Crampin, S., 1994. The fracture criticality of crustal rocks, *Geophys. J. Int.,* **118,** 428–438.

Dvorkin, J. & Nur, A., 1993. Dynamic poroelasticity: a unified model with the squirt and Biot mechanisms, *Geophysics,* **58,** 524–533.

Dvorkin, J., Mavko, G. & Nur, A., 1995. Squirt flow in fully saturated rocks, *Geophysics,* **60,** 97–107.

Endres, A.L. & Knight, R.J., 1997. Incorporating pore geometry and fluid pressure communication into modeling the elastic behaviour of porous rocks, *Geophysics,* **62,** 106–117.

Eshelby, J.D., 1957. The determination of the elastic field of an ellipsoidal inclusion, and related problems, *Proc. R. Soc. Lond.,* A., **241,** 376–396.

Gassmann, F., 1951. Uber die Elastizitat poroser Medien, *Vier. Natur. Gesellschaft Zurich,* **96,** 1–23.

Han, D., 1987. Effects of porosity and clay content on wave velocities in sandstones and unconsolidated sediments, *PhD thesis,* Stanford Univ., CA.

Hill, R., 1965. A self-consistent mechanics of composite materials, *J. Mech. Phys. Solids,* **11,** 213–222.

Hornby, B.E., Schwartz, L.M. & Hudson, J.A., 1994. Anisotropic effective-medium modeling of the elastic properties of shales, *Geophysics,* **59,** 1570–1583.

Hudson, J.A., 1980. Overall properties of a cracked solid, *Math. Proc. Camb. Phil. Soc.,* **88,** 371–384.

Hudson, J.A., 1981. Wave speeds and attenuation of elastic waves in material containing cracks, *Geophys. J. R. astr. Soc.,* **64,** 133–150.

Hudson, J.A., Liu, E. & Crampin, S., 1996. The mechanical properties of materials with interconnected cracks and pores, *Geophys. J. Int.,* **124,** 105–112.

Hudson, J.A., Pointer, T. & Liu, E., 2001. Effective medium theories for fluid saturated materials with aligned cracks, *Geophys. Prosp.,* **49,** 509–522.

Johnston, D.H., Toksoz, M.N. & Timur, A., 1979. Attenuation of seismic waves in dry and saturated rocks: II. Mechanisms, *Geophysics,* **44,** 691–711.

Jones, T., 1986. Pore fluids and frequency-dependent wave propagation in rocks, *Geophysics,* **51,** 1939–1953.

Jones, T. & Nur, A., 1983. Velocity and attenuation in sandstone at elevated temperatures and pressures, *Geophys. Res. Lett.,* **10,** 140–143.

Kelder, O. & Smeulders, D.M.J., 1997. Observation of the Biot slow wave in water-saturated Nivelsteiner sandstone, *Geophysics,* **62,** 1794–1796.
King, M.S., Chaudhry, N.A. & Ahmed, S., 1994. Experimental ultrasonic velocities and permeability of sandstones with aligned cracks, *56th EAGE Meeting, Vienna, Expanded Abstracts,* pp. 3888–3889.
Klimentos, T. & McCann, C., 1988. Why is the Biot slow compressional wave not observed in real rocks?, *Geophysics,* **53,** 1605–1609.
Kuster, G.T. & Toksoz, M.N., 1974. Velocity and attenuation of seismic waves in two-phase media, *Geophysics,* **39,** 587–618.
Mair, K., Main, I.G. & Elphick, S., 2000. Sequential growth of deformation bands in the laboratory, *J. struct. Geol.,* **22,** 25–42.
Mavko, G. & Jizba, D., 1991. Estimating grain-scale fluid effects on velocity dispersion in rocks, *Geophysics,* **56,** 1940–1949.
Mavko, G. & Nur, A., 1975. Melt squirt in the asthenosphere, *J. geophys. Res.,* **80,** 1444–1448.
Mavko, G., Mukerji, T. & Dvorkin, J., 1998. *The Rock Physics Handbook,* Cambridge University Press, Cambridge.
Mochizuki, S., 1982. Attenuation in partially saturated rocks, *J. geophys. Res.,* **87,** 8598–8604.
Murphy, W.F., 1985. Sonic and ultrasonic velocities: theory versus experiment, *Geophys. Res. Lett.,* **12,** 85–88.
Norris, A.N., 1985. A differential scheme for the effective moduli of composites, *Mechan. Mater.,* **4,** 1–16.
Nur, A., 1971. Effects of stress on velocity anisotropy in rocks with cracks, *J. geophys. Res.,* **8,** 2022–2034.
Nur, A., 1980. Seismic velocities in low porosity rocks, in *Source Mechanisms and Earthquake Prediction,* hommage au Professor J. Coulom, CNRS, Paris.
O'Connell, R.J. & Budiansky, B., 1977. Viscoelastic properties of fluid-saturated cracked solids, *J. geophys. Res.,* **82,** 5719–5735.
Peacock, S., McCann, C., Sothcott, J. & Astin, T.R., 1994. Seismic velocities in fractured rocks; an experimental verification of Hudson's theory, *Geophys. Prosp.,* **42,** 27–80.
Plona, T., 1980. Observation of a second bulk compressional wave in a porous medium at ultrasonic frequencies, *Appl. Phys. Lett.,* **36,** 259–261.
Pointer, T., Liu, E. & Hudson, J.A., 2000. Seismic wave propagation in cracked porous media, *Geophys. J. Int.,* **142,** 199–231.
Thimus, J.F., Abousleiman, Y., Cheng, A.H.D., Coussy, O. & Detournay, E., 1998. Poromechanics: a tribute to Maurice A. Biot, *Proc. Biot Conf. Poromechanics, Louvain-La-Neuve, Belgium*. A.A. Balkema, Rotterdam.
Thomsen, L., 1985. Biot-consistent elastic moduli of porous rocks: low frequency limit, *Geophysics,* **50,** 2797–2807.
Tod, S.R., 2001. The effects on seismic waves of interconnected nearly aligned cracks, *Geophys. J. Int.,* **145,** 1–20.
Walsh, J.B., 1969. New analysis of attenuation of partially melted rock, *J. geophys. Res.,* **74,** 4333–4337.
Wang, Z. & Nur, A., 1990. Dispersion analysis of acoustic velocities in rocks, *J. acoust. Soc. Am.,* **87,** 2384–2395.
Wang, Z. & Nur, A., 1992. Elastic wave velocities in porous media: a theoretical recipe, in *Seismic and Acoustic Velocities in Reservoir Rocks,* Vol. 2, *Theoretical and Model Studies.* Society of Exploration Geophysicists, Tulsa.
Winkler, K.W., 1985. Dispersion analysis of velocities and attenuation in Berea sandstone, *J. geophys. Res.,* **90,** 6793–6800.
Winkler, K.W., 1986. Estimates of velocity dispersion between seismic and ultrasonic frequencies, *Geophysics,* **51,** 183–189.
Wu, T.T., 1966. The effect of inclusion shape on the elastic moduli of a two phase material, *Int. J. Solids Structures,* **2,** 1–8.
Zatsepin, S.V. & Crampin, S., 1997. Modelling the compliance of crustal rock. I. Response of shear-wave splitting to differential stress, *Geophys. J. Int.,* **129,** 477–494.
Zhang, J.J. & Bentley, L.R., 2000. Change of elastic moduli of dry sandstone with effective pressure, *70th SEG Meeting, Calgary, Expanded Abstracts,* pp. 1826–1829.

APPENDIX A: MATHEMATICAL BACKGROUND

Eshelby (1957) solved the problem of calculating the deformation of an ellipsoidal elastic inclusion contained in an infinite body of another material when it is subjected to stress and strain fields infinity. His result is that

$$\epsilon_{ij}^{\text{inc}} = T_{ijkl}\epsilon_{kl}^{\infty}, \tag{A1}$$

where ϵ^{∞} is the applied strain field at infinity, ϵ^{inc} is the (uniform) strain field in the inclusion and T_{ijkl} is given by

$$T = [I + SC^{-1}(C^{I} - C)]^{-1}, \tag{A2}$$

where I is the fourth-order identity tensor, C is the elastic stiffness of the matrix, C^{I} is the stiffness of the inclusion and S is a fourth-order tensor defined by Eshelby (1957). The summation convention is assumed throughout this appendix. S depends on the geometry of the inclusion and the Poisson's ratio of the matrix material.

A penny-shaped crack with normal in the x_1 direction is defined to be an ellipsoid with semi-axes a_1, a_2 and a_3 satisfying $a_2 = a_3$ and for which the aspect ratio, $r = a_1/a_2 \ll 1$. Walsh (1969) argues that for such a crack saturated with a fluid of viscosity η, we may assign the fluid a shear modulus of $i\omega\eta$, whereupon

$$T_{1212} = T_{1313} = \frac{\mu/(\mu - i\omega\eta)}{i\omega\eta/(\mu - i\omega\eta) + [(2 - v)/(1 - v)](\pi/2)r}. \tag{A3}$$

We will write

$$T^{s} = 2T_{1212}, \tag{A4}$$

so that

$$\epsilon_{13}^{\text{inc}} = T^{s}\epsilon_{13}^{\infty}. \tag{A5}$$

Zatsepin & Crampin (1997) consider a different, but related problem. In their analysis the inclusion is filled with fluid, the pressure of which is kept constant by an unspecified pumping or draining process independent of the applied stress. They find that the expression for the deformation of the inclusion, ϵ^{inc} may be written as

$$\epsilon^{\text{inc}} = (I - S)^{-1} C^{-1} [\sigma^{\infty} - CSC^{-1} p\delta], \tag{A6}$$

where σ^{∞} is the applied stress field at infinity. This expression may be simplified to give the volume of a crack (or pore), c_v (p_v) in terms of the applied stress, fluid pressure and unstressed volume c_v^0 (p_v^0)

$$c_v = c_v^0 \left(1 - \frac{\sigma_{\text{n}}}{\sigma_{\text{c}}} + \frac{p}{\sigma_{\text{c}}} - \frac{\sigma_{ll}}{3\kappa_{\text{m}}} \right), \tag{A7}$$

$$p_v = p_v^0 \left(1 - \frac{3}{4\mu} \frac{1 - v}{1 + v} \sigma_{ii} + \frac{3}{4\mu} p \right), \tag{A8}$$

where σ_{n} is the normal stress acting on the crack face and

$$\sigma_{\text{c}} = \frac{\pi \mu r}{2(1 - v)} \tag{A9}$$

Zatsepin & Crampin (1997). One can usually neglect the term $\sigma_{ll}/3\kappa_{\text{m}}$ in eq. (A7) in favour of the terms that are $O(1/r)$, to write

$$c_v = c_v^0 \left(1 - \frac{\sigma_{\text{n}}}{\sigma_{\text{c}}} + \frac{p}{\sigma_{\text{c}}} \right). \tag{A10}$$

If we introduce the relationship between the density and the pressure in the fluid:

$$\rho_{\text{f}} = \frac{\rho_0}{1 - p c_{\text{f}}}, \tag{A11}$$

where ρ_0 is the unstressed fluid density and c_{f} is the fluid compressibility, then for small pressure and stress variations the mass in each pore, m_{p}, may be written as

$$m_{\text{p}} = \rho_f p_v = \rho_0 p_v^0 \left[1 - \frac{3}{4\mu} \frac{1 - v}{1 + v} \sigma_{ii} + \left(\frac{3}{4\mu} + c_{\text{f}} \right) p \right], \tag{A12}$$

so that if

$$K_{\text{p}} = \frac{4\mu c_{\text{f}}}{3}, \tag{A13}$$

$$m_{\text{p}}^0 = \rho_0 p_v^0, \tag{A14}$$

we may write this as

$$m_{\text{p}} = m_{\text{p}}^0 + \frac{3 m_{\text{p}}^0}{4\mu} \left[(1 + K_{\text{p}}) p - \frac{1 - v}{1 + v} \sigma_{ii} \right]. \tag{A15}$$

Similarly, we find for cracks:

$$m_{\text{c}} = m_{\text{c}}^0 + \frac{m_{\text{c}}^0}{\sigma_{\text{c}}} [(1 + K_{\text{c}}) p - \sigma_{\text{n}}], \tag{A16}$$

where

$$m_{\text{c}}^0 = \rho_0 c_v^0, \tag{A17}$$

$$K_{\text{c}} = \sigma_{\text{c}} c_{\text{f}}. \tag{A18}$$

Under the assumption of a dilute concentration of cracks and pores, Eshelby (1957) developed an 'interaction energy formula' for calculating the effective elastic constants of composite media. The effective elastic constants C_{ijkl}^{eff} can be written in terms of the elastic tensor of the matrix material, C_{ijkl}, the fractional porosities ϕ_t associated with each type of inclusion and the stress and strain fields in each inclusion as

$$C_{ijkl}^{\text{eff}} \epsilon_{ij}^0 \epsilon_{kl}^0 = C_{ijkl} \epsilon_{ij}^0 \epsilon_{kl}^0 - \sum_t \phi_t \left(\epsilon_{ij}^t \sigma_{ij}^0 - \sigma_{ij}^t \epsilon_{ij}^0 \right), \tag{A19}$$

where the superscript 't' refers to the field in the t th class of inclusion.

APPENDIX B: LIST OF PRINCIPAL NOTATION

Symbol	Meaning	Unit
γ	See eq. (29)	(−)
γ'	See eq. (30)	(−)
ϵ	Crack density	(−)
η	Fluid viscosity	Pa s
θ, ψ	Euler angles	(−)
ι	See eq. (39)	(−)
κ_{f}	Fluid bulk modulus	Pa
λ_{m}, μ, κ_{m}	Reference Lamé parameters	Pa
ρ	Saturated rock density	kg m^{-3}
ρ_0	Fluid density	kg m^{-3}
σ_{c}	$\frac{\pi\mu r}{2(1-v)}$	Pa
τ	Time constant	s
ϕ_{c}	Crack porosity	(−)
ϕ_{p}	Volume fraction of pores	(−)
ω	Frequency	s^{-1}
ς	Grain size	m
a	Crack/pore radius	m
k	Permeability	m^2
l	Wavenumber	m^{-1}
m^*	Fluid mass in individual pore	kg
m_i	Fluid mass in ith crack	kg
p^*	Pressure in pores	Pa
p_i	Pressure in ith crack	Pa
p_v, c_v	Pore, crack volumes	m^3
r	Aspect ratio	(−)
v	Reference Poisson ratio	(−)
C	Elastic stiffness tensor	Pa
K_{c}	$\sigma_{\mathrm{c}}/\kappa_{\mathrm{f}}$	(−)
K_{p}	$4\mu/3\kappa_{\mathrm{f}}$	(−)
$\mathcal{M}$	See eq. (64)	Pa
M	P-wave modulus	Pa
S	Eshelby tensor	(−)